RIGA TECHNICAL UNIVERSITY

Laura Vītola

GEOPOLYMER BINDER FOR THE PRODUCTION OF SUSTAINABLE ALTERNATIVE BUILDING MATERIALS

Summary of the Doctoral Thesis

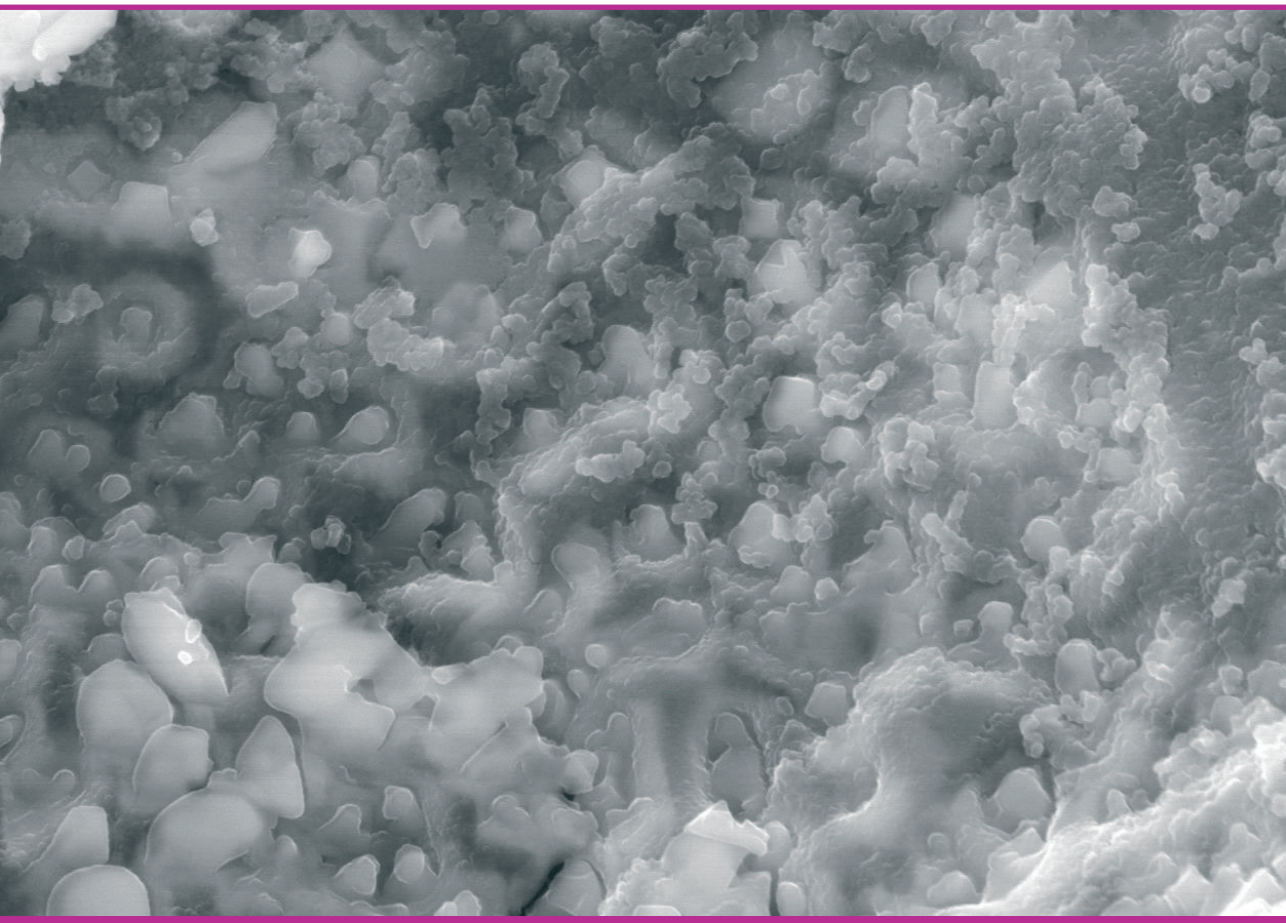

RTU Press
Riga 2023

RIGA TECHNICAL UNIVERSITY
Faculty of Civil Engineering
Institute of Materials and Structures

Laura Vītola
Doctoral Student of the Study Programme "Civil Engineering"

GEOPOLYMER BINDER FOR THE PRODUCTION OF SUSTAINABLE ALTERNATIVE BUILDING MATERIALS

Summary of the Doctoral Thesis

Scientific supervisors
Professor Dr. sc. ing.
DIANA BAJĀRE
Professor Dr. sc. ing.
INA PUNDIENĖ

RTU Press
Riga 2023

Vītola L. Geopolymer Binder for the Production of Sustainable Alternative Building Materials. Summary of the Doctoral Thesis. Riga: RTU Press, 2023. 51 p.

Published in accordance with the decision of the Promotion Council "RTU P-06" of 1st September 2023, No. 04030-9.6.1/6.

Cover picture by Laura Vītola

https://doi.org/10.7250/9789934370069
ISBN 978-9934-37-006-9 (pdf)

DOCTORAL THESIS PROPOSED TO RIGA TECHNICAL UNIVERSITY FOR THE PROMOTION TO THE SCIENTIFIC DEGREE OF DOCTOR OF SCIENCE

To be granted the scientific degree of Doctor of Science (Ph. D.), the present Doctoral Thesis has been submitted for the defence at the open meeting of RTU Promotion Council on 15 December 2023 at 14.15 at the Faculty of Civil Engineering of Riga Technical University, Kipsalas 6A, Room 342.

OFFICIAL REVIEWERS

Asst. Prof., Dr. sc. ing. Sandris Ručevskis
Riga Technical University, Latvia

Asst. Prof., Dr. Sc. Visar Krelani
University for Business and Technology, Kosovo

Asst. Prof., Dr. Patrycja Bazan
Cracow University of Technology, Poland

DECLARATION OF ACADEMIC INTEGRITY

I hereby declare that the Doctoral Thesis submitted for review to Riga Technical University for promotion to the scientific degree of Doctor of Science (Ph. D.) is my own. I confirm that this Doctoral Thesis has not been submitted to any other university for promotion to a scientific degree.

Name Surname ……. (signature)
Date: ……

The Doctoral Thesis has been written in Latvian. It consists of an Introduction, 4 chapters, Conclusions, 52 figures, 10 tables; the total number of pages is 107. The Bibliography contains 219 titles.

CONTENTS

GENERAL DESCRIPTION OF THE DOCTORAL THESIS

Importance of the topic and problem statment

The greatest challenge of our time is climate change and limited resources, and addressing these issues opens the door for a fundamentally new economic model. For this reason, the European Commission approved the Europe's New Sustainable Growth Agenda and the new Circular Economy Action Plan in March 2020 [1]. These are the fundamental provisions of the European Green Deal, a plan to make sure that the climate, energy, transportation, and taxation policies of the European Union (EU) are prepared to reduce greenhouse gas emissions by at least 55 % below the 1990 levels by 2030.

The European Commission intends to make Europe the first region in the world to be carbon neutral, enabling all areas of the EU economy to rise to the challenge and setting up the framework for achieving the climate targets by 2030 in a just, economical, and competitive manner. The Green Deal, the sustainable development plan of the European Commission, has emerged as a significant economic turning point for the world community and, in fact, for all industrial sectors [2]. It is important to consider environmental factors and the effects of newly produced materials on the environment, particularly the crucial concerns of reducing environmental contamination and the conservation and effective use of natural resources [3], [4]. To accomplish the development of a sustainable economy, new technologies and solutions for recycling these reusable raw materials are urgently required since the industrial processes of the war years produce growing amounts of waste materials and byproducts [5]. Research into the recycling of industrial waste and byproducts to produce high value-added products, ranging from agricultural waste materials to plastic trash, is currently being increased [6], [7].

Greenhouse gases (GHG) from materials extraction, building materials production, construction and building renovation are estimated to account for 5–12 % of total EU GHG emissions [8]. Efficient production and use of construction materials could reduce GHG by 80 % [9]. As this sector is responsible for 39 % of energy and process-related emissions and acid rain triggers, the continuation of these greenhouse gas emissions at the same rate is bound to create a critical situation [10]. Therefore, in all efforts related to global climate change and cleaner production, the construction sector must be included as a key player [11].

It is estimated that the production of one tonne of Portland cement produces around one tonne of CO_2 GHG emissions, and that around 2–8 % of global energy consumption is directly attributable to the Portland cement production process [12], [13]. It is therefore vital to implement new alternative materials in the construction sector to ensure sustainability.

Sustainability is mostly discussed from an environmental perspective, but sustainability encompasses several factors, including productivity, economic, environmental, and social impacts [14], [15]. Among the various sustainable materials, geopolymers are being widely studied, as they are able to reduce the environmental impact [16]. Geopolymers as third-generation cements are considered as an environmentally friendly substitute for Portland cement due to their relatively low CO_2 emissions and low combustion/environmental impact

temperatures. Various types of aluminosilicate materials – kaolinite, feldspar, agricultural, industrial, and mining wastes and by-products such as fly ash, ground granulated blast furnace slag, palm oil fuel ash and rice husk ash – can be used as raw materials for the production of geopolymers [17], [18]. Geopolymers are being studied as materials for use in construction because of their relatively high mechanical strength, good volumetric stability (no drying shrinkage) and high resistance to open fire and high temperatures [19]–[21]. However, although they have gained popularity, geopolymers differ in their structural design and technology from traditional building materials (Portland cement and ceramics), making it important to understand the influence of different factors on the properties of geopolymers.

The aim of the Doctoral Thesis

The aim of the research is to develop sustainable alternative building materials with low environmental impact from industrial by-products using geopolymer binder technology.

The tasks of the Doctoral Thesis

1. Develop the geopolymer binder based on secondary raw materials – industrial by-products containing metakaolin.
2. Investigate the effect of activation solution concentration on the properties of fresh geopolymer binders, the physical and mechanical properties of geopolymer binders and the mineralogical composition of the binder. Describe the relationships obtained.
3. Investigate the influence of the manufacturing conditions (temperature and mixing time) on the properties of fresh and cured geopolymer binders. Describe the relationships obtained.
4. Produce porous geopolymer materials and investigate the effect of thermal post-treatment on the physical and mechanical properties, mineralogical composition and structure of the geopolymer binder and on the leaching of OH^- ions. Describe the relationships obtained.
5. Develop a solution to prevent the formation of zeolite crystals in the geopolymer binder, which in the long term may contribute to a reduction in the mechanical strength of the building material. Describe the relationships obtained.
6. Develop a geopolymer binder-based bio-composite and characterise its potential application in construction.
7. Evaluate the sustainability of the developed building materials (binders and bio-composites).

Scientific novelty of the research

The research has led to the development of a new geopolymer binder-based bio-composite in line with the European Green Deal targets, suitable for use in construction. To bring such a product into production, the relationships between the properties of geopolymer binders have been investigated and scientifically elucidated during the Thesis research.

The temperature of the raw materials and the environment and the mixing time of the raw materials are important for the stability of the properties of geopolymer binders. The initial temperature of the geopolymer binder raw materials and the increased water ratio may alter the workability of the fresh geopolymer mortar mix, resulting in material properties (material density, structure, and mechanical strength) of the cured materials that may be significantly different from those expected. Increasing the initial temperature (from 5 °C to 35 °C) and the amount of additional water added can more than double the compressive strength of the geopolymer binder after 28 days of curing.

To optimise the formulation of geopolymer binders and ensure that the final products have the lowest possible environmental impact, it is necessary to select the optimum amount of activation solution and the concentration of alkaline compounds in it. The use of unreasonably high concentrations or excessive amounts of activation solution will not only degrade product properties but will also place undue stress on the environment and contribute to wasteful consumption of resources. During the geopolymerisation process, the unbound activation solution may leach out of the product structure over time, causing not only an unaesthetic appearance of the product but also environmental damage. Therefore, the leaching of OH^- ions from the structure of geopolymer binders depending on the raw material used for its production or the type of aluminium silicate source (i.e., metakaolin or a mixture of metakaolin and fly ash) was investigated.

A method for limiting the formation of zeolites in the geopolymer binder structure has been developed. By varying the silicon content of the activation solution, it is possible to reduce the formation of new zeolite crystals in the geopolymer structure.

Based on the knowledge gained from the studies, bio-composites of the geopolymer binder have been developed using hemp bundles. The result is a self-supporting, low-density (260–400 kg/m^3) thermal insulation material with a compressive strength of up to 0.48 MPa and a thermal conductivity between 0.061 W/(m·K) and 0.077 W/(m·K). The new construction product has been subject to an environmental impact assessment and found to comply with the European Green Deal guidelines.

The practical significance of the Doctoral Thesis

Traditionally, the production of geopolymer binders has been considered as a complex, knowledge-intensive process, easily influenced by human factors. In addition, many countries do not have standards governing the manufacture and use of geopolymers in construction. However, from the perspective of the European Green Deal, geopolymer binders are an ideal solution to ensure the sustainability of construction processes: geopolymer binders have reduced CO_2 emissions compared to traditional binders, geopolymers can use industrial by-products and waste, reducing the consumption of non-renewable resources, geopolymer binders can be produced with reduced energy consumption compared to Protland cement. The production of geopolymer binders from industrial by-products allows the production of binders with early strength (Day 7) in compression up to 48 MPa and in flexure up to 18 MPa, which is equivalent to the strength of conventional binders.

A geopolymer binder bio-composite has been developed using hemp buckets. The result is a self-supporting, low-density (260–400 kg/m^3) thermal insulation material with a compressive strength of up to 0.48 MPa and a thermal conductivity between 0.061 W/(m·K) and 0.077 W/(m·K).

Research methodology

The properties of the raw materials used in the Thesis are characterised by X-ray fluorescence (XRF; PHILIPS PW-1004) and X-ray diffractometry (XRD; BRUKER-AXS D8 ADVANCE).

The viscosity of the fresh binder is determined using an SV-10 vibration meter and the flow rate according to ASTM C 1437. The electrical conductivity is determined using a Mettler-Toledo MPC 227 meter.

The structural development of the geopolymer binder was characterised by ultrasonic pulse velocity (UPV) (Pundit 7). The density and mechanical strength of the material were tested according to EN 1097-6 and EN 196-1. For the characterisation of the mechanical strength, 20 mm × 20 mm × 20 mm specimens tested with the Zwick Z100 universal testing system at a testing speed of 0.5 mm/min were used in separate sections of the study. In the fourth section of the experimental part of the study, the density of the material was determined for prismatic specimens of 10 mm × 10 mm × 60 mm and the mechanical strength was determined according to the Koch-Steinegger method. Water absorption by mass was determined as percentage mass change. Open porosity by volume was calculated as the percentage of the absorbed water volume divided by the dry volume of the sample. A Le Chaternier flask was used to determine the true density of the material, and the total porosity of the material was calculated according to ASTM C188. The pore size distribution was estimated using a Pore Master PM33-12 porosimeter. The mineralogical composition and qualitative phase distribution of the samples were determined by X-ray diffractometry (XRD; BRUKER-AXS D8 ADVANCE), the chemical bonds were characterised by Fourier transform infrared (FTIR; ATIMATTSON FTIR-TM) spectra between 2000 cm^{-1} and 400 cm^{-1}. A JEOL JSM 5400 scanning electron microscope (SEM) with a LINK-ISIS energy dispersive X-ray analyser (EDX) was used for micro-structural and elemental distribution analysis. Thermogravimetric-differential thermal analysis (TG/DTG; Stanton Redcroft STA 781) was performed at 0–700 °C with a heating rate of 5 °C/min. The pH of the geopolymers was determined using a portable pH/mV meter HI 991003. The resulting leachates were titrated to determine the OH^- group (OH^- mol/(L·g)) with 0.01 M HCl.

The bio-fillers used were studied using a Veho Discovery Dx-3 USB digital microscope. Their bulk density was tested by measuring the mass of 3 L buckets packed in a free-falling container from a height of 20 cm. The particle size distribution is expressed in the ranges <1 mm, 1–5 mm, 5–10 mm, 10–15 mm, 15–20 mm, 20–25 mm, 25–30 mm, 30–35 mm, and 35–40 mm. The material density of the bio-composite material was tested according to EN 1602 and the compressive strength at 10 % strain according to EN 826 (Zwick Z100), the thermal conductivity was determined using a Fox 600 heat flow meter. The structure of bio-fillers and

bio-composites was characterised by X-ray computed microtomography (ScancoμCT50). Samples (50 mm × 50 mm × 50 mm) were tested using a sample holder with a diameter of 73 mm and a height of 100 mm.

Range of research

- To obtain geopolymer binders as activation solution using **8–10 M** NaOH solution with sodium metasilicate modification **up to 20 %** by weight.
- To obtain geopolymer binders with a material density of **up to 1500 kg/m^3** and a compressive strength of **at least 8 MPa** after 28 days curing.
- To obtain porous geopolymers with a material density **up to 550 kg/m^3** and a total porosity **up to 79 %** with an OH^- leaching from the structure **not exceeding 0.025 mol/(L·g)** over a period of 35 days.
- Bio-composites with material density **from 260 kg/m^3 to 400 kg/m^3** and compressive strength **up to 0.5 MPa** are obtained for the evaluation of the compatibility of the geopolymer binder and plant-based bio-fillers.

Statements put forward for defence of the Thesis

- The rheology and mechanical strength of a geopolymer binder and the structural properties at constant composition are determined by the initial temperature of the raw materials and the mixing time of the binder.
- Industrial by-products (metakaolin and fly ash) are suitable raw materials for the production of geopolymer binders with mechanical strengths up to 48 MPa in compression and up to 18 MPa in flexure.
- The leaching of the geopolymer binder depends on the raw materials used and can be reduced in the short term by thermal post-treatment.
- By modifying the composition of the geopolymer binder with a metasilicate solution, it is possible to limit the formation of zeolites in the formed geopolymer binder structure, thus preventing a decrease in mechanical strength in the long term.
- The geopolymer binders developed are a sustainable alternative to Portland cement, which can be recommended as a binder for the production of environmentally friendly self-supporting bio-composite products.

Structure and length of the Thesis

The Doctoral Thesis consists of an annotation, an introduction, four main chapters divided into sections, conclusions and a list of references. Chapters 1–3 review the literature, which forms the basis for the formulation of the aim of the dissertation and the tasks to be achieved. Chapter 4 outlines the research methods and materials used, as well as the process of completing the tasks and achieving the objective.

The Thesis contains 107 pages, 54 figures, 12 tables, and a reference list with 219 references. The Thesis is written in Latvian.

Aprobation of the obtained results

The results of the Thesis have been reported and discussed at 9 international conferences. The results obtained during the Doctoral Thesis research have been presented in two publications of conference proceedings and 12 publications of scientific journals, all indexed in SCOPUS database, in total cited 256 times, h_5-index – 7.

The results of the research have been presented at the following international conferences:

1. 6th International Conference "Advanced Construction", Kaunas University of Technology, Lithuania, 20 September 2018.
2. GeopolymerCamp 2019, Geopolymer Institute, France, 8–10 July 2019.
3. 4th International Conference "Innovative Materials, Structures and Technologies" IMST 2019, Riga Technical University, Latvia, 25–27 September 2019.
4. International Scientific Conference "Advanced Construction and Architecture 2020", Kaunas University of Technology, Lithuania, 23–25 September 2020.
5. Riga Technical University 61st International Scientific Conference, Section "Construction Science", Riga Technical University, Latvia, 22 October 2020.
6. 2nd International Symposium on "Sustainable Construction", University of Salerno, Italy, 2–3 October 2021.
7. Riga Technical University 60th International Scientific Conference, Section "Construction Science", Riga Technical University, Latvia, 28 October 2020.
8. 10th UBT Annual International Conference on Civil Engineering, Infrastructure and Environment, University of Business and Technologies, Kosovo, 29–30 October 2021.
9. 5th International Conference "Innovative Materials, Structures and Technologies" IMST 2022, Riga Technical University, Latvia, 28–30 September 2022.

List of publications

1. **L. Vitola**, S. Gendelis, M. Sinka, I. Pundiene, and D. Bajare, "Assessment of Plant Origin By-Products as Lightweight Aggregates for Bio-Composite Bounded by Starch Binder," Energies (Basel), vol. 15, no. 15, Aug. 2022, doi: 10.3390/EN15155330.

2. **L. Vitola**, M. Vilnitis, I. Pundiene, and D. Bajare, "Sustainable building materials based on hemp shives and geopolymer paste," J. Phys. Conf. Ser., vol. 2162, no. 1, p. 012015, Jan. 2022, doi: 10.1088/1742-6596/2162/1/012015.

3. I. Pundiene, **L. Vitola**, J. Pranckeviciene, and D. Bajare, "Hemp Shive-Based Bio-Composites Bounded by Potato Starch Binder: The Roles of Aggregate Particle Size and Aspect Ratio," Journal of Ecological Engineering, vol. 23, no. 2, pp. 220–234, Feb. 2022, doi: 10.12911/22998993/144637.

4. F. Dietrich, P. Łapka, Ł. Cieślikiewicz, P. Furmański, M. Sinka, **L. Vitola,** D. Bajare, "Micro-scale modeling-based approach for calculation of thermal conductivity of bio-based building composite," AIP Conf. Proc., vol. 2429, Nov. 2021, doi: 10.1063/5.0071466.

5. P. P. Argalis, **L. Vitola**, D. Bajare, and K. Vegere, "Alkali-activated zeolite 4A granules-characterization and suitability assessment for the application of adsorption," Crystals (Basel), vol. 11, no. 4, Apr. 2021, doi: 10.3390/CRYST11040360.

6. V. Bocullo, **L. Vitola**, D. Vaiciukyniene, A. Kantautas, and D. Bajare, "The influence of the SiO2/Na2O ratio on the low calcium alkali activated binder based on fly ash," Mater. Chem. Phys., vol. 258, Jan. 2021, doi: 10.1016/J.MATCHEMPHYS.2020.123846.

7. **L. Vitola**, M. Sinka, A. Korjakins, and D. Bajare, "Impact of Organic Compounds Extracted from Hemp-Origin Aggregates on the Hardening Process and Compressive Strength of Different Types of Mineral Binders," Journal of Materials in Civil Engineering, vol. 32, no. 12, 2020, doi: 10.1061/(ASCE)MT.1943-5533.0003461.

8. **L. Vitola**, D. Bajare, A. Palomo, and A. Fernandez-Jimenez, "Low-calcium, porous, alkali-activated materials as novel pH stabilizers for water media," Minerals, vol. 10, no. 11, 2020, doi: 10.3390/min10110935.

9. **L. Vitola**, I. Pundiene, J. Pranckeviciene, and D. Bajare, "The impact of the amount of water used in activation solution and the initial temperature of paste on the rheological behaviour and structural evolution of metakaolin-based geopolymer pastes," Sustainability (Switzerland), vol. 12, no. 19, 2020, doi: 10.3390/su12198216.

10. G. Bumanis, **L. Vitola**, L. Stipniece, J. Locs, A. Korjakins, and D. Bajare, "Evaluation of Industrial by-products as pozzolans: A road map for use in concrete production," Case Studies in Construction Materials, vol. 13, Dec. 2020, doi: 10.1016/J.CSCM.2020.E00424.

11. G. Bumanis, **L. Vitola**, I. Pundiene, M. Sinka, and D. Bajare, "Gypsum, geopolymers, and starch-alternative binders for bio-based building materials: A review and life-cycle assessment," Sustainability (Switzerland), vol. 12, no. 14, Jul. 2020, doi: 10.3390/SU12145666.

12. K. Vegere, **L. Vitola**, P. P. Argalis, D. Bajare, and A. E. Krauklis, "Alkali-activated metakaolin as a zeolite-like binder for the production of adsorbents," Inorganics (Basel), 2019, doi: 10.3390/inorganics7120141.

13. D. Bajare, **L. Vitola**, L. Dembovska, and G. Bumanis, "Waste stream porous alkali activated materials for high temperature application," Front. Mater., vol. 6, Apr. 2019, doi: 10.3389/fmats.2019.00092.

14. S. Moukannaa, M. Loutou, M. Benzaazoua, **L. Vitola**, J. Alami, and R. Hakkou, "Recycling of phosphate mine tailings for the production of geopolymers," J. Clean. Prod., vol. 185, pp. 891–903, Jun. 2018, doi: 10.1016/J.JCLEPRO.2018.03.094.

CONTENT OF THE THESIS

1. European policy framework

In 1987, the Brundtland Commission defined the new concept of "sustainable development". The report published by the Commission, Our Common Future [22], defines the term as follows:

"Sustainable development is development that meets the needs of the present without compromising the ability of future generations to meet their own needs."

Over the years, this concept has become a guiding principle for politics and economics. Thus, "sustainable development" must be addressed in industry, construction, agriculture, energy, transport, and other human activities [23].

Activities related to construction and public projects are the single largest cause of natural resource consumption in Europe (i.e., 31 %) [24]. The construction sector faces four main challenges: greenhouse gas (GHG) emissions, energy consumption, reducing the use of non-renewable resources, and waste management and recycling. Overall, three broad objectives of sustainable construction have been identified to ensure sustainable construction practices (i.e., resource conservation, cost optimisation and human-centred design) [25].

In March 2020, the European Commission (EC) adopted a new Circular Economy Action Plan and a new Sustainable Growth Agenda for Europe to build a climate-smart economy [1]. These are the key documents of the European Green Deal, which aims to ensure that the European Union's (EU) climate, energy, transport, and tax **policies are ready to reduce greenhouse gas emissions by at least 55 % below 1990 levels by 2030.** The EC's sustainable development programme, the Green Deal, has become a major economic milestone for the global community and, indeed, for all industries [2].

The EC aims to transform Europe into a global climate neutral leader and to require all sectors of the EU economy to meet their climate targets in a fair, cost-effective and competitive way by 2030. Reducing the overuse and waste of natural resources and promoting sustainable growth are the key to achieving the EU's 2050 climate neutrality targets and stopping biodiversity loss [26]. The circular economy is an integral part of the new EU industrial strategy. A recent study shows that applying circular economy principles across the EU economy could increase EU gross domestic product (GDP) by an additional 0.5 % by 2030, creating around 700,000 new jobs [27].

The construction sector provides ~9 % of EU GDP, as well as direct (18 million) and indirect job opportunities [28]. The construction sector consumes around 50 % of the world's raw materials and 36 % of its energy, generating more than 35 % of all waste generated in the EU [10], [29].

Sustainable construction is therefore a key objective of the EU's Circular Economy policy – a regenerative economy that reduces the negative environmental impacts of the construction sector. One way to achieve this is to promote the environmentally friendly

production of building materials, using local resources, reducing energy and water consumption, using waste and production by-products as raw materials [30].

2. Environmental impacts of the construction sector

Building materials are essential to modern society, but their production is clearly linked to increased GHG emissions. The production of various materials has increased GHGs from 5 Gt CO_2 equivalent in 1995 to 11 Gt in 2015, i.e., a percentage increase from 15 to 23 % of the increase in global emissions [9]. For the purposes of this calculation, materials are "solid materials", including metals, wood, structural materials, and plastics. Most of the emissions associated with materials extraction and production come from bulk materials: iron and steel (32 %), cement, lime, and gypsum (25 %), plastics and rubber (13 %), etc. (see Fig. 2.1)The construction and industrial product groups each account for 40 % of the GHG emissions from global materials production.

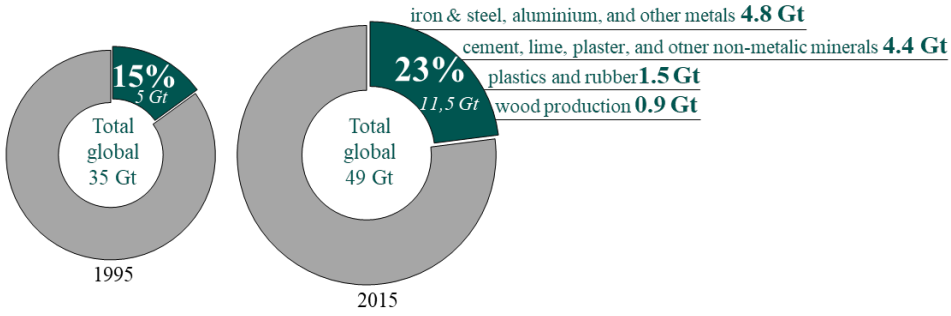

Fig. 2.1. Emissions from building materials production processes compared to the total emissions for the period 1995–2015 [9].

The production of construction materials has a significant impact on the environment, from the extraction of raw materials to the disposal of the finished product at the end of its life cycle. **To reduce the negative environmental impact of the production of construction materials**, a combination of the following strategic steps is needed: (i) **use sustainable raw** materials that are renewable, recyclable or bio-degradable; (ii) **reducing the amount of waste produced** by recycling or reusing production waste to protect the environment and save money; (iii) **optimising energy consumption** by optimising energy-intensive production processes and using renewable energy; (iv) **assessing the life cycle of materials,** considering the environmental impact of materials throughout their life cycle; (v) **applying environmentally friendly standards** to industrial buildings; (vi) **educating the society, including professionals (e.g., architects, producers, designers, construction managers)**.

According to the International Energy Agency's 2017 data, the largest part of the construction sector's emissions come directly from the operation of buildings, i.e., 28.0 %. Meanwhile, 22.7 % of emissions come from concrete, steel, and aluminium production, and 20.3 % from industry (materials production) [31].

3. Innovative building materials with reduced environmental impact

By using low-carbon or carbon-neutral materials, incorporating alternative materials, and using advanced technologies, the building sector can make significant progress in reducing GHG emissions and reducing climate change. Most traditional building materials have an increased negative impact on the environment during their life cycle. For example, familiar insulation materials such as glass wool, rock wool, extruded polystyrene foam, and polyurethane foam cause significant environmental damage both during the production process and at the waste disposal stage [32].

Due to increasing environmental concerns as well as the depletion of natural resources, geopolymer binders are seen as a valuable alternative to Portland cement. Compared to Portland cement, the world's most widely used binder, both the extraction and the geopolymerisation of geopolymer binders have up to 80 % lower CO_2 emissions [33]. Several researchers have highlighted the potential of geopolymers for the production of sustainable building materials [34]–[37]. L. N. Assi et.al. have summarised the available literature on geopolymers as sustainable materials and potential alternatives to conventional Portland cement [36]. Geopolymers can be made from commercially available feedstocks as well as from lower quality materials, industrial waste, and by-products (e.g., fly ash, blast furnace slag, etc.), demolition waste and other types of waste [38]. Geopolymer binder is a relatively new inorganic binder synthesised by mixing a reactive (i.e., amorphous, or vitreous) powder containing aluminium silicates with an alkaline activation solution and curing at elevated temperatures (approximately 60 °C to 90 °C) for a certain period of time.

Bio-composites containing plant-based fillers, such as hemp or flax shive, have become increasingly popular in the construction sector as primary building materials over the last decades, as they provide an environmentally and human-friendly environment [39], [40]. One of the most common bio-composite materials used in construction is lime and hemp bio-composite, which consists of by-products of industrial hemp production, i.e., hemp shive and lime binder. During growth, hemp absorbs CO_2 by photosynthesis and carbon is sequestered in the lime by carbonation, resulting in a carbon neutral or even negative material that stores up to 130 kg CO_2 ekv/m^3 [41].

New plant-based bio-composites with mineral binders offer potentially improved physical, mechanical and thermal properties, low environmental impact, and recyclability [42]. The use of a geopolymer binder for bio-composites might allow variations in material properties depending on the type of amorphous aluminium silicate source used and the composition of the activation solution [43]. Leaching is the main cause of geopolymer neutralisation. The alkalinity of geopolymer mortars is much easier to reduce, regardless of external conditions, compared to Portland cement mortars [44]. This is common in bio-composite materials, which can lead to leaching of alkalis from the geopolymer matrix and interaction with bio-fillers.

4. Experimental part

In the experimental part of the Thesis, geopolymer binders based on metakaolin obtained as a by-product of industrial production were produced, to which fly ash and synthetic zeolite additives were added in separate sections of the study. Their properties in fresh and cured state have been investigated. The preparation of porous high-performance binders with a pore-forming additive was carried out and the structural stability and OH^- leaching were investigated. Under laboratory conditions, zeolite additives synthesised from industrial by-products were added to the geopolymer binder, the effect of zeolite additives on the mechanical and structural properties of the geopolymer binder was investigated, and the way in which the development of zeolites in the binder structure can be controlled by an appropriate activation solution was determined. A feasibility study has been carried out on the compatibility of the geopolymer binder with the bio-filler hemp bagasse.

Raw materials

In this study, metakaolin powder (MK), obtained as an industrial by-product from the production of other materials, was used as a source of aluminium silicate to produce geopolymers. The most intense crystalline phase of MK is quartz minerals, while the specific surface area is 892 m^2/kg. MK consists of thin lamellar particles ranging in size from 1 μm to 20 μm. The main constituents of the MK are SiO_2 (46.10–53.74 %) and Al_2O_3 (37.2–44.47 %), Fe_2O_3 (0.45–1.10 %), CaO (0.20–0.21 %), K_2O and Na_2O (0.55–0.70 %), TiO_2 (0.10–0.70 %), MgO (0.10–0.20 %), and other compounds (0.38–13.8 %), LOI at 1000 ºC 0.20–1.00 %.

Fly ash (FA) was obtained in Spain from the Teruel thermal power plant, which uses coal as fuel. Before using FA, it was ground in a ball mill for 30 min, 75 % of FA < 45 μm. According to XRD, the fly ash is composed of glassy phase aluminium silicates and contains small amounts of crystalline phases such as mullite ($Al_6Si_2O_{13}$), hematite (Fe_2O_3), and quartz (SiO_2). FA consists of SiO_2 (39.03 %), Al_2O_3 (27.06 %), Fe_2O_3 (19.5 %), CaO (6.40 %), K_2O and Na_2O (1.20 %), TiO_2 (0.96 %), MgO (1.04 %), and other compounds (4.81 %), LOI at 1000 ºC 2.25 %.

The alkaline medium for the reactions was provided by activation solutions. The main component of the activation solution is sodium hydroxide flakes (Tianye Chemicals Ltd.) dissolved in a certain amount of water to obtain a solution of a certain molarity. In the first section of the study, 10M NaOH solution has been used as the base activation solution, but in the other parts of the study, 4 activation solutions have been used, respectively A1 (8 M NaOH solution), A2 (8 M NaOH solution, 10 % replaced by sodium metasilicate solution), A3 (8 M NaOH solution, 20 % replaced by sodium metasilicate solution), and A4 (sodium metasilicate solution, 10 % replaced by NaOH flakes).

The additives used for the geopolymer binder are synthesised zeolites obtained under laboratory conditions: zeolite additive C1 derived from fly ash and zeolite additive C2 derived from metakaolin. NaOH solution was added to the metakaolin and fly ash to ensure crystallisation of the zeolites. The zeolites C1 and C2 were obtained by conventional

hydrothermal synthesis. The obtained zeolite powder was washed, filtered, and then dried at 45 ºC. The resulting C1 contains crystals of the zeolite P1 ($(Na_6Al_6Si_{10}O_{32}\cdot 12H_2O$). C2 is a non-homogeneous structure with crystals of different size and shape, containing pseudo-cubic crystals which are considered to be crystals of zeolite 4A ($Na_{96}Al_{96}Si_{96}O_{384}\cdot 6H_2O$, Si/Al = 1) [45], and cambial crystals which are hydroxyl-sodalite $Na_{1,08}Al_2Si_{1,68}O_{7,44}\cdot 1{,}8H_2O$, Si/Al = 0.8) crystals [46]. Both P1 and 4A are among the most widely used zeolites [47]–[49] and are also the most common by-products of geopolymerisation [50]–[52]. The main use of zeolites 4A is for the exchange of Na^{2+} with Ca^{2+} in aqueous media and for the adsorption of gas impurities in reactors. P1 zeolites have a relatively high ion exchange capacity and can therefore be used to recover radioactive elements, heavy metals, and other environmentally undesirable compounds from wastewater treatment.

Two commercially available bio-fillers have been used for the bio-composites: HS-A – commercially available hemp shive grown and processed in Lithuania and obtained from "Natural Fibre" Ltd, and HS-B – commercially available hemp shive grown and processed in Latvia and obtained from "Latgale Agricultural Science Centre" Ltd. HS-A consists of longer particles (up to 40 mm in the longest dimension), while HS-B consists mainly of particles with a longest dimension of 25 mm. HS-B is dominated by particles of the 1–15 mm fraction (88.8 %), but HS-A is composed of 50.8 % particles of the 1–15 mm fraction and the largest particles account for 33.4 % of the composition. The hemp blades used have a bulk density of 80 kg/m^3 and a thermal conductivity of 0.043 W/(m·K) (HS-A) and 0.045 W/(m·K) (HS-B).

Test methods

The chemical composition of the powdered raw materials is analysed by X-ray fluorescence (XRF) determined on a PHILIPS PW-1004 X-ray spectrometer. Their mineralogical composition and qualitative phase distribution are determined using a BRUKER-AXS D8 ADVANCE X-ray diffractometer. Diffractograms are taken with CuKα1, α2 radiation in the range 5–60º (2Θ).

The viscosity of the fresh binder is determined using a vibration viscometer SV-10 to 12000 mPa/s with an accuracy of 0.01 mPa/s. The flowability is determined immediately and after 10 min and 20 min after mixing using the mini-slump test according to ASTM C 1437. The electrical conductivity of the fresh binder is determined using a Mettler-Toledo MPC 227 meter (EC electrode InLab 730.0 mS/cm – 1000 mS/cm range).

The structural development of the geopolymer binder is evaluated by the ultrasonic pulse velocity (UPV) method using a Pundit 7 instrument.

The material density and compressive strength are tested in accordance with EN 1097-6 and EN 196-1. In the second section of the experimental part of the study, the compressive strength of 6 parallel specimens (20 mm × 20 mm × 20 mm) of each geopolymer binder composition is tested on Days 3 and 28 using different mixing times. The specimens are tested using a Zwick Z100 universal testing system (ZwickRoell) at a testing speed of 0.5 mm/min. In the fourth section of the experimental part of the study, the material density is determined for

prismatic specimens of 10 mm × 10 mm × 60 mm and the mechanical strength is determined according to the Koch-Steinegger method [53].

Water absorption by mass is determined as the percentage change in mass of dry samples after complete immersion in water for seven days [54]. A Le Chaterier flask is used to determine the true density, and the total porosity of the material is calculated according to ASTM C188. The pore size distribution is estimated using a Pore Master PM33-12 porosimeter.

The samples have been pulverised at the determined age and their mineralogical composition and qualitative phase distribution determined using a BRUKER-AXS D8 ADVANCE X-ray diffractometer. Diffractograms are taken with CuKα1, α2 radiation in the range 5–60º (2Θ). The chemical bonds in the obtained binders have been characterised by Fourier transform infrared (FTIR) spectra obtained with an ATIMATTSON FTIR-TM spectrometer in the range 2000 to 400 cm^{-1}. FTIR samples have been prepared by mixing 300 mg of KBr with 1 mg of the test binder. A JEOL JSM 5400 scanning electron microscope (SEM) with a LINK-ISIS energy dispersive X-ray analyser (EDX) is used to analyse the microstructure and elemental distribution of the geopolymer binder. Thermogravimetric-differential thermal analysis (TG/DTG) is performed using a Stanton Redcroft STA 781 thermal analyser 0–700 °C at a heating rate of 5 °C/min.

To characterise the pH of the geopolymers in aqueous media and leaching, geopolymer granules with a diameter of 2–4 mm (3.0 ± 0.2 g) were immersed in 100 ml deionised water for 24 h. The samples were transferred to a new dose of deionised water (100 ml) every 24 h. A portable pH/mV meter HI 991003 with sensor check was used to determine the pH of the leachates. The resulting leachates were titrated to determine the OH^- group (OH^- mol/(L·g)) with 0.01 M HCl solution to pH 7.0.

A Veho Discovery Dx-3 USB digital microscope has been used to visually assess the bio-fillers. A 3 L vessel (standard vessel for testing concrete aggregates) filled with particles free-falling from a height of 20 cm is used to determine the bulk density of the bio-aggregates.

The bio-fillers used are studied using a Veho Discovery Dx-3 USB digital microscope. Their burial density has been tested by measuring the mass of 3 litre buckets packed in a free-falling container from a height of 20 cm. The particle size distribution is expressed in the ranges <1 mm, 1–5 mm, 5–10 mm, 10–15 mm, 15–20 mm, 20–25 mm, 25–30 mm, 30–35 mm, 35–40 mm. The density of the bio-composite material is tested according to EN 1602, the compressive strength at 10 % strain according to EN 826 (Zwick Z100) and the thermal conductivity is determined using a Fox 600 heat flow meter. The structure of bio-fillers and bio-composites is characterised by X-ray computed microtomography (ScancoμCT50). Samples are tested using a 73 mm diameter and 100 mm height sample holder scanned at 70 μA.

4.1.The impact of the temperature and activation solution on the properties of the geopolymer binder

The industrial-scale adoption of geopolymer-based materials and products in the construction sector can significantly improve the sustainability of the construction industry. In

order to promote the industrial acceptance of materials, it is important to identify the key parameters that can significantly influence the workability and properties of a geopolymer-based fresh binder. This is particularly important on construction sites where temperatures can change rapidly during the day or vary widely depending on the season. The properties of the activation solution and the geopolymerisation reactions are directly dependent on temperature. The initial temperature of the geopolymer binder and the addition of water to the formulation may alter the workability of the fresh mix, resulting in different properties of the cured materials than expected.

Given that constant conditions are often not sufficiently addressed or not possible in construction and other manufacturing plants, this section of the study investigates the effect of temperature and activation solution concentration on the properties of fresh and cured geopolymer binder.

Preparation of samples

The geopolymer binder samples are prepared according to the compositions given in Table 4.1. The ratio of metakaolin (MK) to 10 M NaOH is constant for all compositions (1.00/0.25). The activation solution (AS) is prepared by adding distilled water to 10 M NaOH and stirring for 30 min with a magnetic stirrer.

First, all the starting materials have been kept at 5 °C, 15 °C, 25 °C, and 35 °C for 24 h. The geopolymer binders are prepared at room temperature, i.e., +20 ± 2°C, by stirring for 3 min with a mechanical stirrer at 140 rpm. The physical and mechanical properties of the three selected compositions (MK0.6, MK1.0, and MK1.4) have been determined. The prepared binders have been filled into metalic moulds (70 mm × 70 mm × 70 mm) covered with polyethylene film to ensure humidity and immediately placed in a preheated climate chamber at 80 °C for 24 h. During the curing, the UPV of the samples has been determined. After 24 h of curing in the climate chamber, the samples have been exposed, labelled and measured, and the samples continued to cure at room temperature, i.e., +20 ± 2°C.

Table 4.1

Mixture design of produced samples

Composition	Raw materials, mass part			Water / 10M NaOH	Total solution molarity	Liquid / MK
	Metakaolin (MK)	10M NaOH	Waters			
MK0.6	1.00	0.25	0.15	0.6	8.7	0.40
MK0.8			0.20	0.8	8.3	0.45
MK1.0			0.25	1.0	8.0	0.50
MK1.2			0.30	1.2	7.7	0.55
MK1.4			0.35	1.4	7.4	0.60
MK1.6			0.40	1.6	7.1	0.65
MK1.8			0.45	1.8	6.9	0.70

Results

The viscosity of both the 10 M NaOH solution and distilled water depends directly on the temperature of the respective liquids (see Fig. 4.1). Increasing the temperature from 5 °C to 35 °C causes a significant (i.e., fivefold) decrease in the viscosity of the 10 M NaOH solution

(i.e., from 33.0 mPa·s till 6.5 mPa·s). For distilled water, the viscosity decreases twice as the temperature is increased from 5 °C to 35 °C.

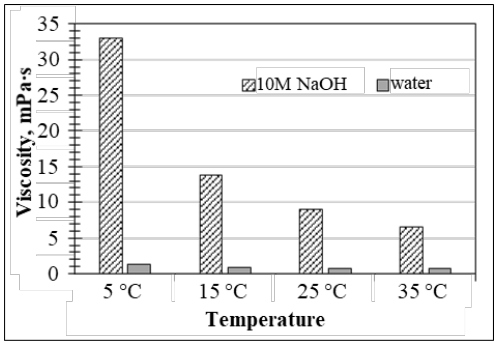

Fig. 4.1. Viscosity of 10 M NaOH solution and distilled water at different temperatures.

In order to evaluate more objectively the effect of activation solution temperature on the properties of the geopolymer binder, the electrical conductivity and viscosity of fresh geopolymer binders have been determined (see Fig. 4.4).

Diluting a 10 M NaOH solution with distilled water increases the degree of dissociation, which in turn causes an increase in electrical conductivity (see Fig. 4.2 a)). Increasing the water/10 M NaOH solution ratio increases the electrical conductivity of the geopolymer binder. The dissolution process is affected by temperature, i.e., increasing the temperature of the solution increases the number of ions in solution and increases the degree of dissociation caused by the activation of the electrolyte molecular bonds [193]. As the bonds become more flexible, they are more easily ionised, resulting in a higher concentration of ions in solution. The data show that the electrical conductivity of the geopolymer binder is significantly affected by the binder temperature. Geopolymer binders with the lowest initial temperature (i.e., 5 °C) have the lowest electrical conductivity. Increasing the water/10 M NaOH solution ratio (from 0.6 to 1.8) decreased the ionic content of the binder by 30 % and increased the electrical conductivity of the binder from 90 mS to 120 mS. The highest increase in electrical conductivity was found for the binders containing a higher water/10 M NaOH solution ratio, so the amount of water in the geopolymer binder plays a role in increasing its electrical conductivity.

As can be seen in the graph (Fig. 4.2 b)), the viscosity of the geopolymer binder decreases with increasing water/10 M NaOH solution ratio. Consequently, a correlation between the electrical conductivity and viscosity of the geopolymer binder can be observed. A higher viscosity of the geopolymer binder leads to a lower ionic mobility and consequently a lower electrical conductivity [60]. The highest viscosity is observed for a geopolymer binder with an initial temperature of 5 °C. A significant decrease in viscosity (i.e., approximately a factor of two, from 350 mPa·s to 170 mPa·s) is observed for geopolymer binders with a water/10 M NaOH solution ratio of 0.6 to 1.2, respectively. The viscosity of the geopolymer binder increases with increasing NaOH concentration in the activation solution. This is due to the higher OH^- concentration [61]. If the water/10 M NaOH solution ratio is greater than 1.2, the decrease in viscosity of the binder is negligible.

Increasing the initial temperature of the binder also increases the ionic mobility and electrical conductivity of the activation solution [62], which causes an increase in the degree of dissociation in the solution, resulting in a decrease in the viscosity of the solution and the degree of hydration of the ions. The viscosity of the geopolymer binder decreases as the initial temperature of the binder increases. Since the water/10 M NaOH solution ratio and the initial temperature of the binder affect the ionic concentration and viscosity, these parameters can be used to control the workability of the geopolymer binder.

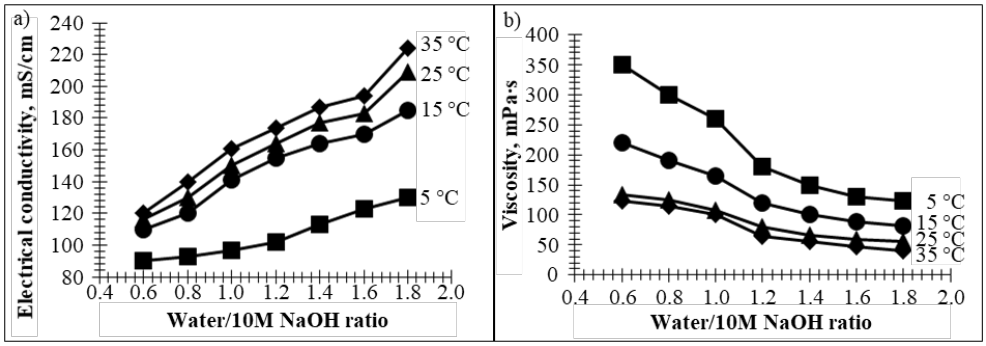

Fig. 4.2. Impact of water/10 M NaOH solution ratio on the properties of a geopolymer binder: a) electrical conductivity; b) viscosity.

Another parameter of the workability of a binder is the flowability, which is determined by a mini-slump test and is related to the flow stress and plastic viscosity of the binders [63], [64]. Increasing the water/10 M NaOH solution ratio causes an increase in the spread diameter (see Fig. 4.3), and this behaviour is observed regardless of the initial temperature of the geopolymer binder. The values of the spread diameter of the geopolymer binder depend on the electrical conductivity and viscosity of the binder. The smallest spread diameter (10.4–16.0 mm depending on the water/10 M NaOH solution ratio) is observed for the geopolymer binder with an initial temperature of 5 °C (see Fig. 4.3). At 10 min and 20 min after the incorporation of the geopolymer binder, the behaviour of the binder spread diameter as a function of the water/10 M NaOH solution ratio remained unchanged. A significant increase in the spread diameter is observed when the temperature of the geopolymer binder was increased to 25 °C and 35 °C (Fig. 4.3 c) and d)). Increasing the water/10 M NaOH solution ratio has a significant effect on increasing the electrical conductivity and viscosity of the geopolymer binder (Figs. 4.2) and increases the spread diameter of the geopolymer binder. At a water/10 M NaOH solution ratio of 1.8, the spread diameter of the geopolymer binder at 25 °C and 35 °C was 16–20 cm, respectively, which is too high for optimum incorporation of the geopolymer binder.

The optimum outlet diameter of the geopolymer binder for quality embedment is 14 cm. Geopolymer binders with lower alkali concentrations in the formulation may have difficulty in embedding due to their relatively high flowability. There is a clear behaviour towards a decrease in the spread diameter of the geopolymer binder over time (10 min and 20 min after binder incorporation). This indicates that the formation of primary geopolymer gel structure is more intense in binders with higher initial temperatures (25 °C and 35 °C) and thus higher electrical

conductivity during the first 20 min after mixing. Optimal flowability is observed for the geopolymer binder with a higher water/10 M NaOH solution ratio and lower initial temperature (i.e., 5 °C and 15 °C), but by increasing the initial temperature of the geopolymer binder (i.e., to 25 °C and 35 °C) optimal flowability can be achieved by reducing the water/10 M NaOH solution ratio.

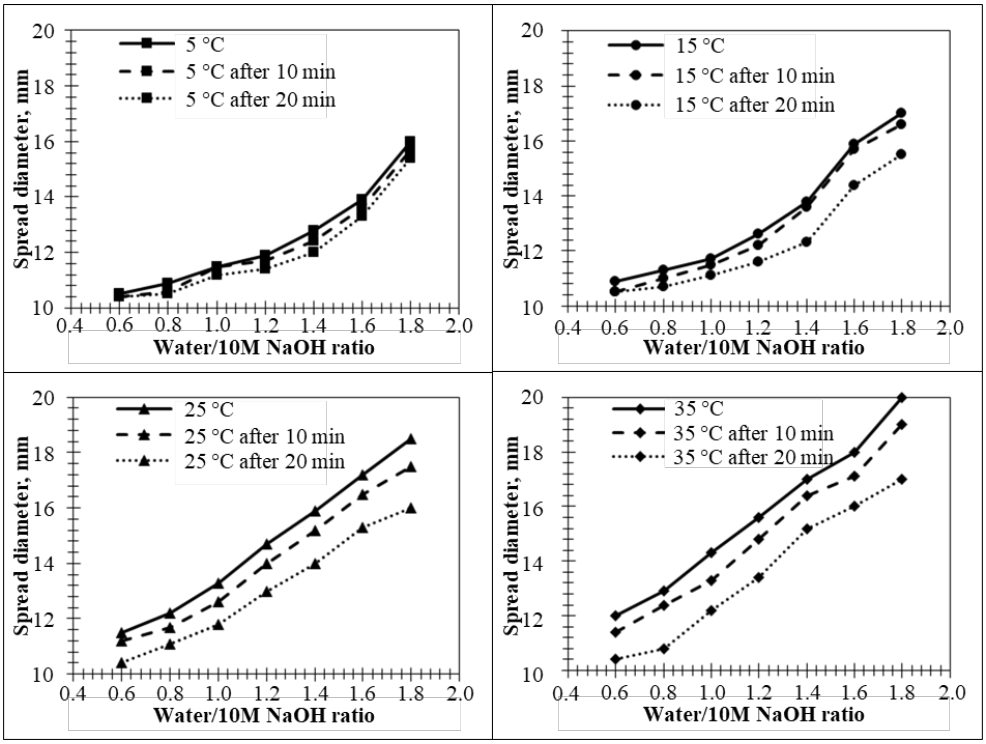

Fig. 4.3. Impact of water/10 M NaOH solution ratio on the flowability of the geopolymer binder immediately, 10 min and 20 min after binder mixing; a) initial geopolymer binder temperature 5 °C; b) initial geopolymer binder temperature 15 °C; c) initial geopolymer binder temperature 25 °C; d) initial geopolymer binder temperature 35 °C.

The time evolution of the geopolymer binder structure has been characterised using UPV and depends on the water/10 M NaOH solution ratio and the initial binder temperature (see Fig. 4.4). As the water/10 M NaOH solution ratio decreases, the ultrasonic pulse of the geopolymer binder moves faster in the material structure. Increasing the initial temperature of the geopolymer binder from 15 °C to 35 °C after the first 2 h of curing at 80 °C increases the UPV values 1.5–1.8 times. Apparently, this is due to the higher electrical conductivity (Fig. 4.2), accelerating the geopolymerisation reactions. After four to 6 h of curing at elevated temperatures, a significant change is observed for the geopolymer binder with the lower water/10 M NaOH ratio. The UPV increases threefold to 1359 m/s for M0.6-35, 880 m/s for M0.6-15 and 720 m/s for M0.6-5. For the geopolymer binder with a higher water/10 M NaOH solution ratio (i.e., 0.14), the UPV is significantly lower: 600 m/s (M1.4-5), 430 m/s (M1.4-35)

and 330 m/s (M1.4-15). Not only the increased amount of water in the activation solution used for the geopolymer binder, but also the low initial temperature of the geopolymer binder has a negative effect on structure formation, prolonging structure formation and leading to lower UPV values. By selecting the optimum initial geopolymer binder temperature and water/10 M NaOH solution ratio it is possible to reduce the curing time of the samples at elevated temperatures.

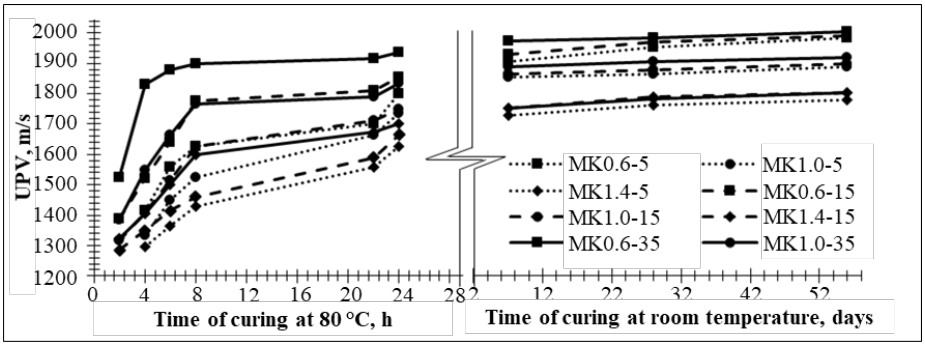

Fig. 4.4. Ultrasonic pulse velocity (UPV) changes in time of geopolymer binders with different water/10 M NaOH solution ratios and different initial binder temperatures.

Mercury porosimetry is used to characterise the porosity of the geopolymer binder (Fig. 4.5). The pore size distribution has been determined for four compositions: M0.6-5 and M0.6-35, as well as M1.4-5 and M1.4-35. According to the results obtained (Fig. 4.5), the pores of M0.6-5 are mainly in three diameter ranges: 0.01 μm to 0.1 μm, 0.3 μm to 0.5 μm and 1.0 μm to 4.0 μm. The total pore volume of M0.6-5 reaches 0.280 cm^3/g. In contrast, M0.6-35, made at a higher initial temperature of 35 °C, has only two predominant pore diameter ranges: 0.01 μm to 0.1 μm and 0.3 μm to 0.5 μm. The total pore volume of M0.6-35 reaches 0.267 cm^3/g. It can therefore be concluded that as the initial temperature of the geopolymer binder increases, the overall porosity decreases, as does the proportion of pores with diameters >1 μm. As can be seen from the graphs, the predominant pore size ranges for M1.4-5 can be divided as follows: 0.05 μm to 0.5 μm and 0.8 μm to 8 μm. The total pore volume of the geopolymer binder M1.4-5 reaches 0.381 cm^3/g, which is 36 % higher than the total pore volume of M0.6-5. Meanwhile, M1.4-35 has a total pore volume of 0.358 cm^3/g, which is 44 % higher than M1.4-5. A higher water/10 M NaOH solution ratio in the geopolymer binder then results in a higher overall porosity of the geopolymer binder and a larger predominant pore size. The higher pore size and pore volume are closely related to the viscosity of the fresh binder.

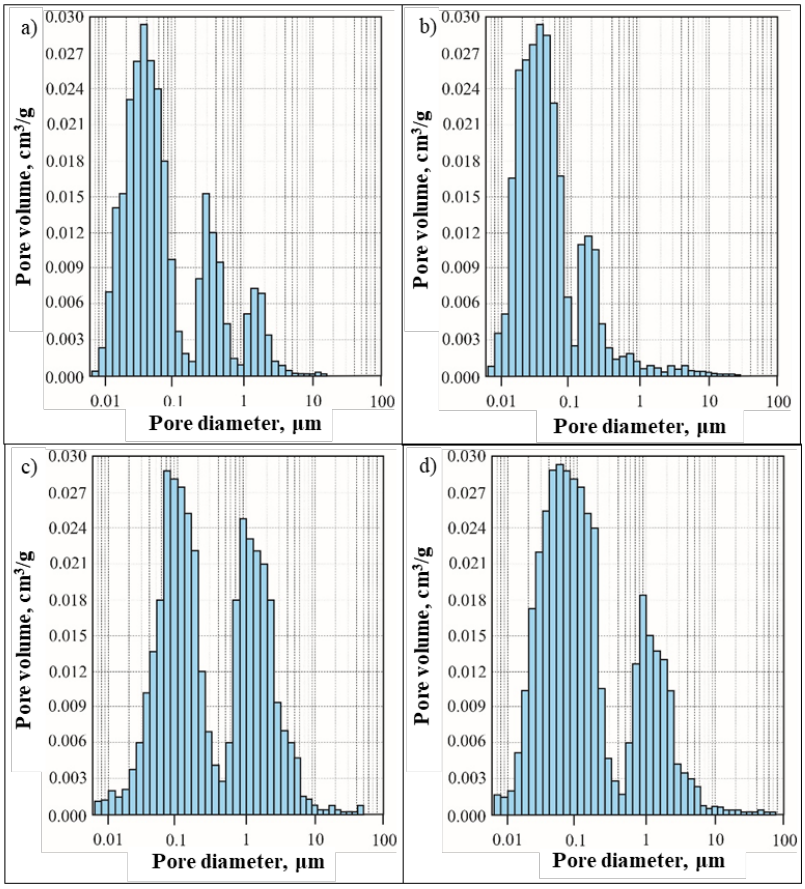

Fig. 4.5. Pore size distribution of the geopolymer binder: a) M0.6-5; b) M0.6-35; c) M1.4-5; d) M1.4-35.

4.2. Effect of binder mixing time on the properties of geopolymer binders

The requirements for geopolymer materials vary from industry to industry. For example, geopolymer materials used in construction must have good adhesion to aggregates and reinforcement and be able to withstand a variety of impacts on them (e.g., mechanical and chemical impacts). As geopolymer-based materials and products become more and more popular and attractive from an industrial production point of view, it is essential to have a better understanding of the main factors influencing the properties of this material during its production. As the structure and synthesis of geopolymers differ significantly from traditional building materials (e.g., Portland cement and ceramic manufacturing technology), it is necessary to investigate the influence of various factors, such as the type of activation solution, on the final material properties. One of the most typical and commonly used geopolymer activation solutions is NaOH-based activation solutions. By modifying NaOH solutions with

sodium metasilicate solution, it is possible to influence the material's workability and the properties of the cured material.

This section of the study investigates the influence of the type of activation solution (i.e., sodium hydroxide solution and sodium metasilicate solution modified sodium hydroxide solution) and the mixing time of fresh binder on the properties of fresh and cured geopolymer binders.

Preparation of samples

Three series of geopolymer binders (3 mixtures per series) have been studied (see Table 4.2), metakaolin (MK) has been mixed with three activation solutions (A1, A2, and A3, respectively) using 3 different activation solution/metakaolin (AS/MK) ratios of 0.5, 0.6, and 0.7. The activation solutions were prepared and kept at room temperature (20 °C ± 2 °C) for 3 h before the geopolymer binder was made. The powdered FC was dosed and mixed with a certain amount of the selected activation solution according to Table 4.2. The samples were stirred for 1, 3, 5, and 7 min to evaluate the effect of the stirring time. Immediately after mixing, the moulds (20 mm × 20 mm × 20 mm) were filled with the prepared geopolymer binder and the flowability of the geopolymer binder was determined in parallel. The samples were placed in sealed plastic bags and kept at room temperature (20 °C ± 2 °C) for 1 h, after which they were cured at 85 °C for 24 h. After reconstitution, the samples were further cured at room temperature (20 °C ± 2 °C) until Day 3, when a portion of the samples was tested, and the remaining samples were then further cured in air and water media at room temperature (20 °C ± 2 °C) until Day 28.

Table 4.2

Mixture design of produced samples

Composition	Raw materials, mass part					Main oxides, %			Main oxides ratios, masas %		
	Metakaolin (MK)	Activation solution (AS)			AS/MK	SiO_2	Al_2O_3	Na_2O	SiO_2 / Al_2O_3	SiO_2 / Na_2O	Al_2O_3 / Na_2O
		A1	A2	A3							
MK-0-0.5	1.0	0.5			0.5	38.2	23.8	13.4			
MK-0-0.6	1.0	0.6			0.6	35.8	22.3	12.5	1.6	2.9	1.8
MK-0-0.7	1.0	0.7			0.7	33.7	21.0	11.8			
MK-10-0.5	1.0		0.5		0.5	40.2	23.8	14.0			
MK-10-0.6	1.0		0.6		0.6	37.7	22.3	13.1	1.7	2.9	1.7
MK-10-0.7	1.0		0.7		0.7	35.4	21.0	12.4			
MK-20-0.5	1.0			0.5	0.5	42.1	23.8	14.7			
MK-20-0.6	1.0			0.6	0.6	39.5	22.3	13.8	1.8	2.9	1.6
MK-20-0.7	1.0			0.7	0.7	37.2	21.0	13.0			

Results

To characterise the flowability of the geopolymer binder, the dispersion diameter of the fresh binder has been determined and the results are shown in Figure 4.6.

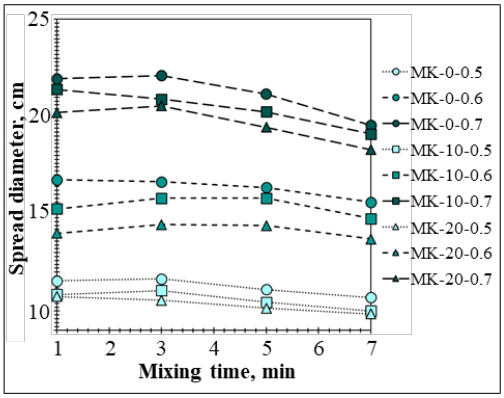

Fig. 4.6. Spread diameter of fresh geopolymer binder depending on the mixing time.

The spread diameter of geopolymer binders with an AS/MK ratio of 0.5 ranges from 9.85 cm to 11.65 cm, with an AS/MK ratio of 0.6 from 13.70 cm to 16.65 cm and with an AS/MK ratio of 0.7 from 18.30 cm to 22.10 cm, depending on the type of activation solution and the duration of mixing. As activation solutions A2 and A3 are obtained by modification of an 8 M NaOH solution with a sodium metasilicate solution, both A2 and A3 have a higher viscosity compared to activation solution A1. This contributes to the different fluidity between binders with the same AS/MK ratio but different activation solutions. The additional metasilicate solution in the activation solution reduces the fluidity of the fresh binder. The effect of mixing time on the fluidity of the geopolymer binder depends on the AS/MK ratio: as the AS/MK ratio increases, the effect of mixing time becomes more significant.

The resulting geopolymer binder presents material density between 1303 kg/m^3 and 1552 kg/m^3 depending on the composition and the mixing time of the fresh binder. The material density depends on the AS/MK ratio as well as on the type of activation solution used.

The results for the compressive strength of the geopolymer binder are shown in Fig. 4.7. The samples for each composition (Table 4.5) were tested on Day 3 (after air curing) and on Day 28 (after air curing and after water curing).

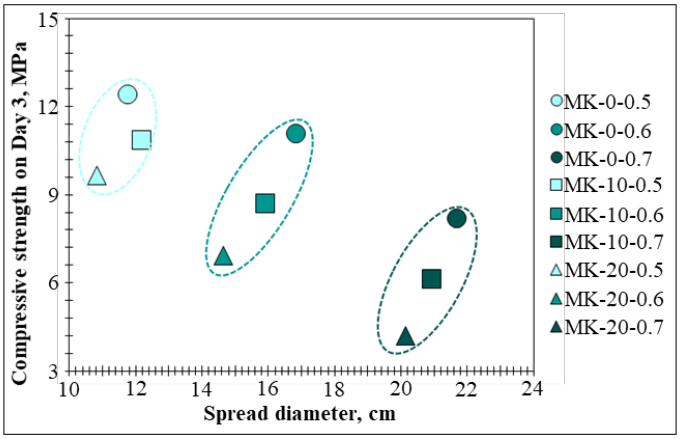

Fig. 4.7. Correlation between flowability (spread diameter) of fresh geopolymer binder and compressive strength after curing on Day 3.

Geopolymer binders were obtained with compressive strengths at Day 3 ranging from 3.6 MPa to 13.5 MPa. Comparing all three series, it can be argued that the addition of sodium metasilicate to the 8M NaOH solution reduces the compressive strength on Day 3 to 22.7 % when 10 % of the 8M NaOH solution is replaced by sodium metasilicate and even to 53.4 % when 20 % of 8M NaOH is replaced by sodium metasilicate. The sodium metasilicate solution consists of Na_2O, reactive (or amorphous) SiO_2 and H_2O, all three of which are required for the geopolymerisation reaction. As shown in Table 4.2, the different AS/MK ratios do not change the ratio of the major oxides but affect the total amount of major oxides in the composition. Higher amounts of reactive silica and sodium in the geopolymer binder can lead to the formation of zeolites as by-products of the reaction, thus damaging the structure of the material during crystal formation; zeolites and geopolymer gel require the same major oxides and zeolites can form faster than geopolymer gel, thus less major oxides are available for the geopolymerisation reaction.

According to the obtained results, fresh geopolymer binders must be mixed for at least 3 min. It can be concluded that the geopolymer binder made with activation solution A1 (8M NaOH) shows the highest compressive strength and the geopolymer binders with an AS/MK ratio of 0.7 show the highest flowability, which is important for workability, e.g., during bio-composite production.

4.3. Leaching of geopolymer binders

When a building material comes into contact with its environment (air, water, etc.), it is possible that the more unstable compounds in its structure can engage in chemical reactions. In the case of geopolymer binder-based products, there is a risk that the material structure contains free alkali compounds which, when in contact with water, may leach onto the surface of the material. The long-term behaviour of the materials must be clearly predictable to be used in construction.

This section of the study investigates the leaching of geopolymer binders into the aquatic environment over a long period of time and develops recommendations to limit leaching. As the binder is relatively dense, the surface area of the geopolymer binders was increased by adding the pore-forming additive hydrogen peroxide (H_2O_2) to characterise the leaching. By increasing the surface area, free alkali can more easily escape from the material structure and the effect of variables on free salinity can be more accurately determined, minimising the influence of measuring instruments and human error on the results.

Preparation of samples

To fully evaluate the maximum degree of leaching, a pore-forming additive has been added to the geopolymer binder to increase the surface area. Hydrogen peroxide (H_2O_2) has been used as the pore forming additive. The compositions produced can be seen in Table 4.3. Two compositions were produced: one based on metakaolin, and one based on a mixture of metakaolin and fly ash.

Table 4.3

Mixture design of produced samples

Composition	Raw materials, mass part				Main oxides, mass %				ratio		
					from aluminium silicate source		from activation solution				
	metakaolin (MK)	fly ash (FA)	activation solution (A2)	pore-forming additive	SiO_2	Al_2O_3	Na_2O	SiO_2	SiO_2/Al_2O_3	SiO_2/Na_2O	Al_2O_3/Na_2O
MK_0	1.0	0.0	0.92	0.015	[a]27.77 [c]19.92	[a]22.98 [c]17.31	[b]8.73	[b]1.28	[a]1.26 [c]1.23	[a]3.33 [c]2.43	[a]2.63 [c]1.98
FA+MK_0	0.4	0.6	0.57	0.015	[a]28.43 [c]23.60	[a]21.58 [c]14.42	[b]6.60	[b]0.97	[a]1.36 [c]1.70	[a]4.45 [c]3.72	[a]3.27 [c]2.18

a – from bulk composition; b – from activator; c – reactive oxide concentration determined by acid attack [65].

All raw materials had been kept at +5 °C for 24 h before sample preparation to slow down the reaction between H_2O_2 and the activation solution and to allow additional time for the binder to be mixed and placed in the moulds. The ratio of activation solution to solids (AS/S) has been chosen according to the results of previous studies to find the optimum consistency of fresh binder to ensure complete incorporation of H_2O_2 into the formulation and maximum porosity of the resulting material. The amount of activation solution used varies for the aluminium silicate source (i.e., metakaolin or a mixture of metakaolin and fly ash) to ensure optimum binder workability. As shown in Table 4.3, the AS/S ratio for the metakaolin-based geopolymer binder is 0.92, whereas for the geopolymer binder based on a mixture of metakaolin and fly ash it is 0.57, which is due to the different granulometry and morphology of the source material particles.

First, the powdered raw materials are dosed and homogenised, and then an appropriate amount of activation solution is added. The mixture is stirred with a mechanical hand mixer for 1.5 min on low speed and 1.5 min on high speed. After a homogeneous binder paste is obtained,

the pore forming additive H_2O_2 is added, and the mass is mixed for a further 10 seconds at low speed. The resulting binder is immediately filled into moulds (40 mm × 160 mm × 160 mm), covered with polyethylene film, and left at room temperature (20 °C ± 2 °C) for 30 min while the H_2O_2 reacted, and the material formed a porous structure.

The samples cured for 20 h at 85 °C. After curing, half of the samples have been heat treated (i.e., heated at 200 °C for 3 h) to investigate the effect of elevated temperature on the leaching of the samples. The specific temperature (200 °C) has been chosen based on the results of previous studies. Monolithic cubes (40 mm × 40 mm × 40 mm) and pellets (2–4 mm) of the samples obtained before and after heat treatment were prepared. The cubic samples have been obtained using a sawing machine, and the pellets have been obtained by mechanical grinding and sieving through 2 mm and 4 mm sieves. After the mechanical test, the samples have been powdered for further tests (i.e., true density, XRD, FTIR, and DTA/TG tests).

Results

In this section, porous geopolymers with material densities of 460–550 kg/m^3, water absorption up to 60 % and total porosities in the range 76–79 % have been obtained. As shown in Table 4.4, the material density of the geopolymer decreases after heat treatment, although no volumetric changes are observed for the samples. Therefore, the change of material density as a result of the heat treatment is attributed to the evaporation of free water in the material structure or degradation of hydration products, as discussed further in the study under DTA/TG results. The water absorption of the metakaolin-based geopolymers (MK-0) is 58 % ± 1 %, while for the samples containing a mixture of metakaolin and fly ash (MK + FA-0) as a source of aluminium silicates it is close to 53 % ± 4 %.

Table 4.4

Physical properties and compressive strength of produced samples

Composition	Material density, kg/m^3	Water absorption, %	Open porousity, %	Total pourosity, %	Compr. strength on Day 3, MPa	Compr. strength on Day 10*, MPa
MK-0	490 ± 15	58 ± 1	29 ± 2	77 ± 2	0.41 ± 0.04	0.46 ± 0.03
MK-200	460 ± 8	60 ± 1	32 ± 1	79 ± 1	0.41 ± 0.03	0.49 ± 0.04
MK+FA-0	550 ± 17	53 ± 4	25 ± 1	76 ± 1	0.73 ± 0.05	0.82 ± 0.05
MK+FA-200	520 ±15	59 ± 3	28 ± 1	77 ± 1	1.03 ± 0.02	1.21 ± 0.04

** Samples cured in air for the first three days, in water for the last 7 days.*

As shown in Table 4.4, the compressive strengths of the porous geopolymers on Day 3 vary from 0.4 MPa to 1.0 MPa, depending on the type of aluminium silicate source and heat treatment. The heat treatment does not affect the compressive strength at Day 3 of the metakaolin-based porous geopolymers, both MK-0 and MK-200 have a compressive strength at Day 3 of 0.4 MPa. Ten day old samples cured in water for the last seven days show a 12–20 % increase in compressive strength. For materials intended to be in contact with water during service, it is vital that the water environment does not reduce their mechanical strength. As the results show an increase in strength, it can be assumed that the geopolymer structure continues to evolve as water dissolves the free alkali in the structure and thus promotes its reaction with unreacted AlO_4^- and SiO_4^{2-} [66].

The macrostructure of the porous geopolymers before heat treatment is shown in Fig. 4.8. As can be seen in the figure, the samples are characterised by a non-homogeneous porous structure with a maximum diameter of up to 2.00 mm.

As can be seen in Fig. 4.9, different types of crystals can be detected on the porous surface. In the MK_0 sample, irregular dodecahedral crystals with diameters ranging from 3.0 μm to 7.0 μm are found in the pore surface. The mineralogical composition of these crystals could not be determined by XRD, probably due to their size and low concentration. According to literature data [67], these crystals are defined as analcite crystals. The surface of the MK + FA_0 pore is covered by deformed cubic crystals with a diameter of 1.5–20 μm (defined as zeolite 4A) and spherical crystals with a diameter of 1.0–3.0 μm, defined as chabazite according to the XRD results.

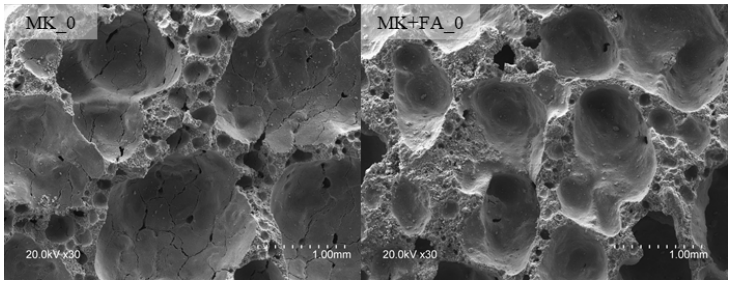

Fig. 4.8. The macro-structure of the obtained porous geopolymers investigated by SEM at 30 times magnification.

The TG/DTG analysis has been performed to characterise the effect of temperature on the porous geopolymers produced. The resulting TG/DTG curves of the geopolymers are shown in Fig. 4.10. The graph focuses on the changes observed between 25 °C and 200 °C; the peak of the DTG curve at 129 °C reflects the water loss of MK_0, which accounts for 11.5 % of the mass loss, and 8.9 % for MK+FA_0 at 127 °C, respectively. The mass loss of the geopolymers between 25 °C and 150 °C is due to the evaporation of physically bound water from the porous structure [68] and to the different ratios of activation solution to dry starting material used in the sample preparation. MK_0 contains 1.5 times more water coming from the activation solution than MK+FA_0.

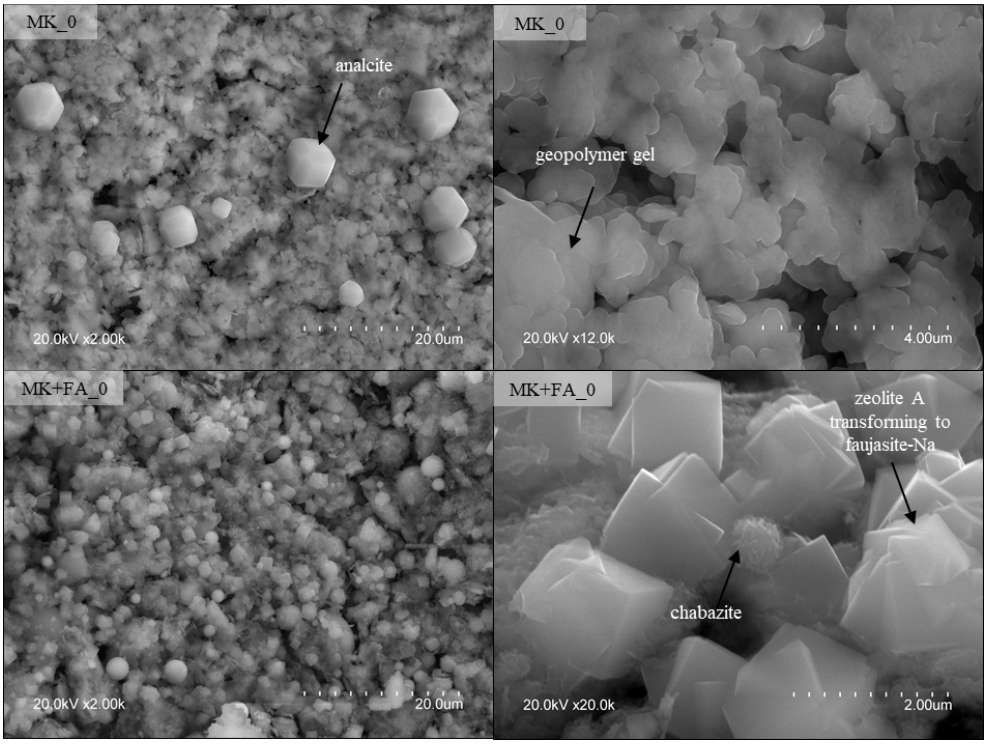

Fig. 4.9. Microphotographs of the pore surface of the obtained porous geopolymers.

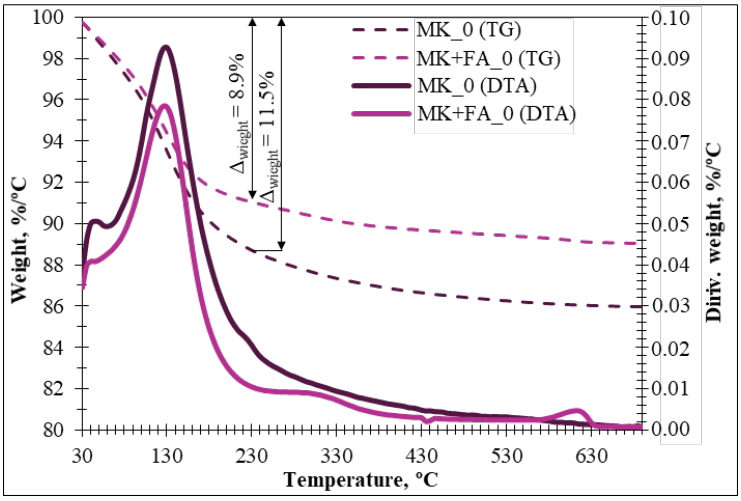

Fig. 4.10. TG/DTG analysis of the obtained porous geopolymers.

The results of the leaching test show that the obtained geopolymer achieves pH ≥ 10 for up to 30 days (see Fig. 4.11). The metakaolin-based geopolymers provide a continuous decrease in pH up to Day 30 in aqueous media (i.e., from pH 11.1 to 10.5), the metakaolin and fly ash

blend-based geopolymers show very similar results, pH 11.4 (Day 1) and decreasing to 10.5 on Day 30. Heat treatment during the test period (30 days) has no effect on the leaching of the geopolymers. According to Table 4.3, it can be stated that the samples based on metakaolin contain 1.5 times less alkali than the samples based on a mixture of metakaolin and electrostatic precipitators, and the presence of different types and amounts of zeolites is observed in the samples (Fig. 4.9). During the first days of the test, the pH is maintained by the free alkali in the pore solution; as the free alkali decreases, the pH in the aqueous medium is maintained by the zeolites and geopolymer gel present in the structure, thus ensuring a gradual release of alkali from the material structure.

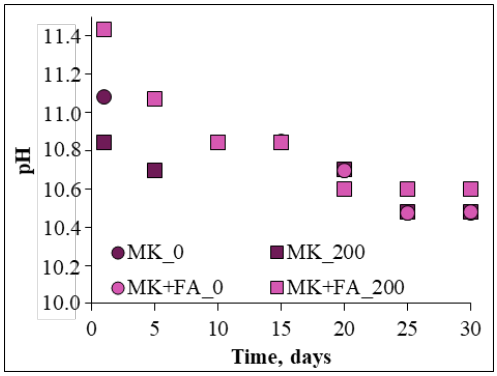

Fig. 4.11. The pH changes of the obtained porous geopolymers in aqueous media over time.

As shown in Fig. 4.12, the heat treatment affected the leaching properties of the samples, depending on the composition (Table 4.3). The amount of OH^- ions leached from the geopolymer structure depended on the type of aluminium silicate source (metakaolin or mixture of metakaolin and fly ash) used as a starting material for the samples. After 30 days of leaching MK_0 leaches 0.019 OH^- mol/(L·g), while MK + FA_0 leaches 0.025 OH^- mol/(L·g) (Fig. 4.12 a). The chemical composition of the aluminium silicate sources provides different SiO_2/Al_2O_3 ratios (Table 4.3), which may affect the leaching of OH^- from the material structure.

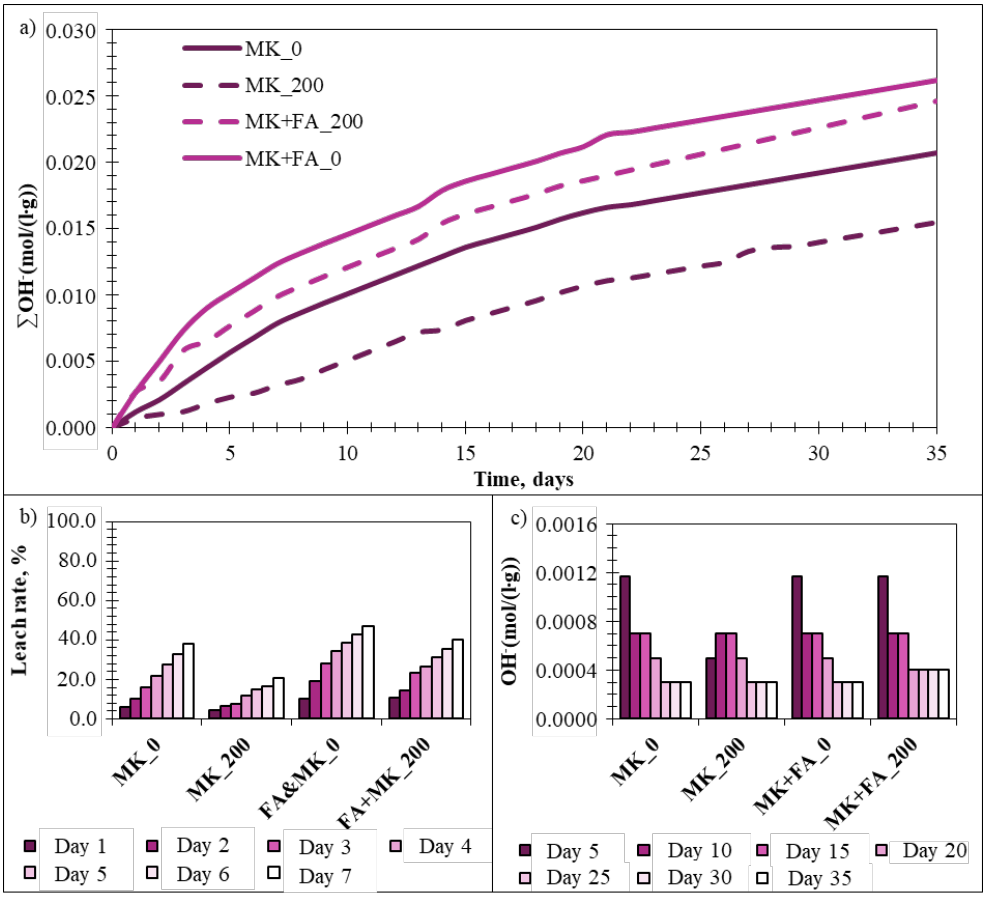

Fig. 4.12. a) The cumulative leaching rate of OH^- ions; b) OH^- ions leached in the first testing week compared to the total leached OH^- ions over 35 days; c) the total amount of OH^- per each 5 test days.

A significant effect of heat treatment on leaching properties (Fig. 4.12) was found for the metakaolin-based samples. Comparing the amount of leached OH^- over a 30-day period, it decreases by 26 % (i.e., from 0.019 mol/(L·g) to 0.014 mol/(L·g)) in the heat-treated samples, but the pH correction in aqueous media remains similar (Fig. 4.28). This means that the pH correction efficiency is higher in the heat treated samples and, given that the amount of alkali used to prepare the samples is the same, the correction will be longer lasting compared to the untreated samples. MK + FA_0 and MK + FA_200 showed an 8 % reduction in the total leached amount of OH^- ions: 0.025 (MK + FA_0) mol/(L·g) – 0.023 (MK + FA _200) mol/(L·g) after 30 days in aqueous media.

Leaching of OH^- from the geopolymer structure after heat treatment at 200 °C for the first week is less intense; it is uniform and lasts longer, which is important if the material needs to be prepared for a stable pH environment. According to Figs. 4.12 a) and 4.12 c), the leaching

of metakaolin-based geopolymers may continue after a period of 30 days and is close to linear in nature.

The increased amount of leached OH^- ions depends not only on the presence of free alkali (i.e., Na^+) in the material structure, but also on the zeolites and geopolymer gel formed during the geopolymerisation process. The test results show that zeolites 4A and analcite can prolong and even out the leaching of OH^- ions over time; MK_0 and MK + FA_0 show a more equivalent rate of OH^- leaching over 30 days. In addition to the chemical composition, the formation of zeolite can also be controlled by pressure, temperature, synthesis time and pH of the activation solution [71]. In this case, the time, temperature, and pressure are constant for all samples, but the amount of sodium silicate is different. The raw materials (chemical and mineralogical composition) influence the type of zeolites formed during geopolymerisation. The effect of heat treatment on leaching depends mainly on the amount of activation solution, leaching depends largely on the chemical composition of the samples.

4.4. Formation and evolution of zeolites in geopolymer structure

Geopolymers are similar in properties to natural zeolite minerals – unlike zeolite minerals, the geopolymer gel is semi-amorphous. If crystals of zeolites start to form in the geopolymer gel under certain conditions, the mechanical properties of the geopolymer binder can be significantly reduced, not only during the curing process but also during the lifetime of the geopolymer product. As the zeolite crystals grow and reach a critical size, internal stresses are generated and the structure of the geopolymer materials can be weakened or even destroyed. The formation of zeolites in the structure of geopolymer materials has been relatively well studied, but there is less research on the conditions that limit the formation of zeolites. It is known that the formation of zeolites depends on the composition of the geopolymer binder and the curing conditions, and different zeolites can be formed in the geopolymer binder structure, such as Na-A, hydroxyl dodalite, zeolite X, fauhasite, etc. [72]–[76]. There are no clear-cut methods to control and limit the formation of zeolites in geopolymers, so it is not possible to guarantee that the properties of the geopolymer binder remain constant over time.

In this section, the formation of zeolites in a geopolymer binder is initiated by adding artificially synthesised zeolites, which act as crystallisation centres in the material structure, and by providing conditions maximally favourable for the development of zeolite crystals. The aim is to identify the reasons for the enhanced development of zeolites in the geopolymer binder structure.

Preparation of samples

Table 4.5 shows the geopolymer compositions produced in this section of the study. All raw materials used were stored at +5 ºC for 24 h before sample production. The ratio of activation solution to dry starting material of 0.92 was chosen in accordance with the results of previous delight studies to ensure optimum consistency and incorporation of fresh geopolymer binder. As shown in Table 4.5, two batches of samples have been produced: a low-silica activation solution A2 (8 M NaOH solution, of which 10 % has been replaced by sodium metasilicate

solution) and a high-silica activation solution A4 (sodium metasilicate solution, of which 10 % has been replaced by NaOH flakes).

Table 4.5

Mixture design of produced samples

Composition	Raw materials, mass part				
	metakaolin (MK)	zeolite		activation solution	
		P1	4A	A2	A4
M-R-A2	1.0			0.92	
M-P-A2	0.9	0.1		0.92	
M-A-A2	0.9		0.1	0.92	
M-R-A4	1.0				0.92
M-P-A4	0.9	0.1			0.92
M-A-A4	0.9		0.1		0.92

First, the dry raw materials were dosed and the powder mixtures are homogenised. Then the appropriate activation solution was added and the mixture mixed slowly for 1.5 min and rapidly for 1.5 min with a mechanical hand mixer. After obtaining a homogeneous paste, it was formed into moulds (10 mm × 10 mm × 60 mm) which, after filling, were covered with a polyethylene film and left at room temperature (20 ± 2 °C) for 30 min. The moulds placed on 2 cm high spacers were then placed in closed containers filled with water to ensure 100 % humidity. The closed containers were kept in a drying oven at 85 ºC for 20 h to ensure curing of the geopolymers without rapid evaporation of water from the porous structure and favourable conditions for the zeolites. After curing, the containers were removed from the oven, opened and left until they reached room temperature of 20 ± 2 ºC (i.e., ~1 h). Then, the samples were demoulded and labelled. The geopolymer samples were kept in a climate chamber (+20 ºC and 100 % humidity).

Results

Geopolymer binders with material densities ranging from 1230 kg/m^3 to 1670 kg/m^3 have been obtained (see Fig. 4.13). As shown in the graph, the amount of silica in the activation solution has an effect on the material density, while the zeolite additives have no effect on the material density.

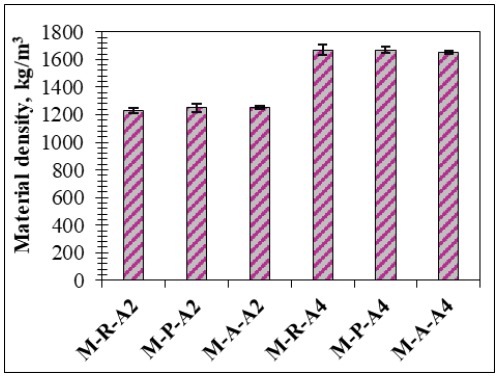

Fig. 4.13. Material density of the obtained geopolymer binder.

Similarly, the type of activation solution also affects the strength characteristics. The compressive strength ranges from 10 MPa to 48 MPa, while the flexural strength ranges from 3 MPa to 18 MPa (Fig. 4.14). Although the addition of C1 and C2 does not have a significant effect on the material density of the resulting geopolymer binder, there is an effect on the compressive strength. As shown in Fig. 4.14, the addition of zeolites to the geopolymer binder causes a decrease in compressive strength when using activation solution A2 (low silica), but the addition of C1 causes an increase in compressive strength when using activation solution A4 (high silica). Since C1 also acts as a filler in the case of M-P-A2 and M-P-A4, so that the MK and C1 particles can form a denser structural "package".

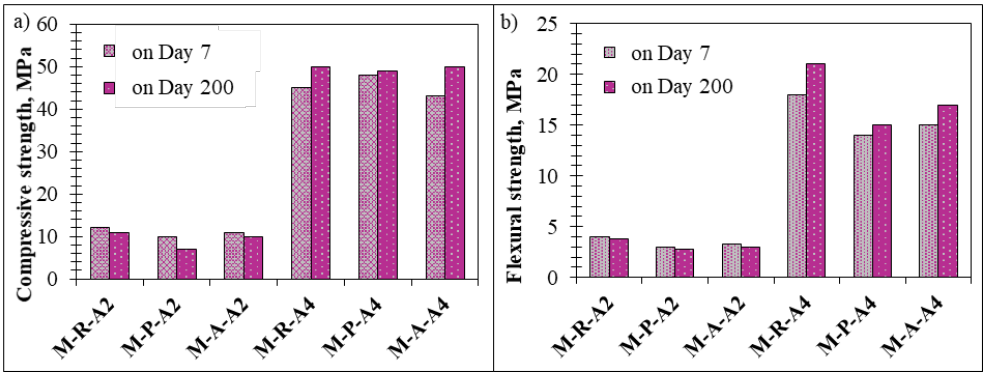

Fig. 4.14. Compressive strength and flexural strength of obtained geopolymer binders.

As shown in Fig. 4.14, the samples produced with the A2 activation solution present a compressive strength of 10 MPa to 12 MPa on Day 7, while the samples produced with activation solution – 43 MPa to 48 MPa. The effect of the zeolite additive on the compressive strength is relatively insignificant, but the compressive strength can be increased up to four times by changing the activation solution.

The flexural strength, like the compressive strength, depends mainly on the activation solution used. As shown in Fig. 4.14, the flexural strength of the geopolymer binder with activation solution A2 is between 3 MPa and 4 MPa, while the geopolymer binder made with

activation solution A4 has a flexural strength of 14–18 MPa on Day 7. Although the addition of C1 to the geopolymer binder with activation solution A4 contributes to a slight increase in compressive strength, the results show a decrease in flexural strength.

XRD was used to characterise the geopolymerisation results. All X-ray diffractograms show elevations of 20–30 degrees on a 2Θ scale (Fig. 4.15). The elevation in the metakaolin diffractogram of 15–25 degrees is characteristic of amorphous aluminium silicates. It shifts to the left as a result of geopolymer gel formation [77]. According to the diffractograms obtained, geopolymerisation has occurred in all geopolymer binder compositions.

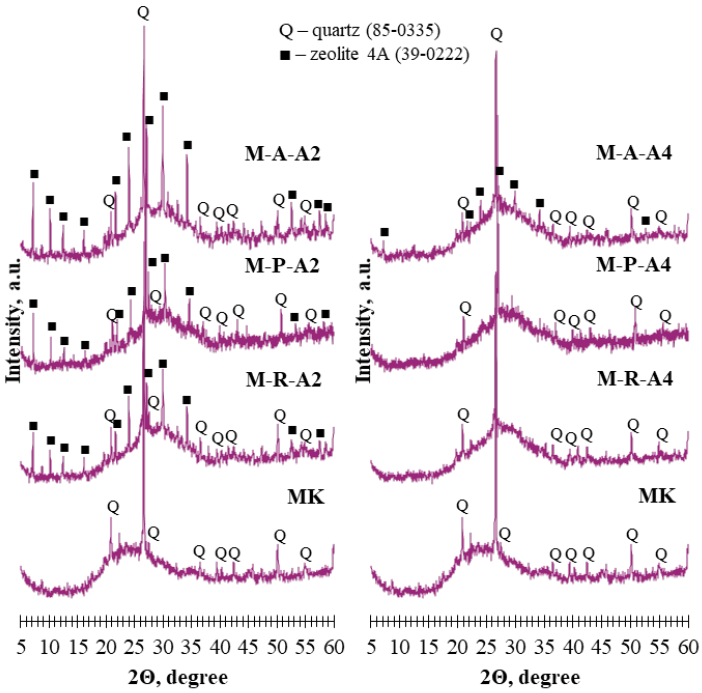

Fig. 4.15. X-ray diffractograms of the obtained geopolymer binders: a) with low-silica activation solution (activation solution A2); b) with high-silica activation solution (activation solution A4).

Metakaolin is characterised by an amorphous phase and crystalline SiO_2 or quartz (Fig. 4.15). As can be seen from the diffractograms, the mineralogical composition depends on the type of activation solution usedThe reference composition M-R-A2 contains zeolites 4A ($Na_{96}Al_{96}Si_{96}O_{384}$-$6H_2O$), but the reference composition M-R-A4 does not form new crystalline compounds during geopolymerisation according to X-ray diffractometry.

Zeolites 4A are observed in M-P-A2, while no effect of P1 on the mineralogical composition is observed. However, A4 influences the mineralogical composition, as shown in Fig. 4.15, in the geopolymer binder with added 4A (i.e., M-A-A2), the formation of zeolite 4A is more intense during the geopolymerisation process than in the reference sample M-R-A2. In

this case, the zeolites in 4A act as crystallisation centres, and thus the 4A in M-A-A2 contributes to the more intense development of crystalline phases. The use of activation solution A4, i.e., with a high silicon content, prevents the formation of reaction by-products or new crystalline compounds during the geopolymerisation process.

The presence of zeolites in the composition may improve the mechanical strength of the geopolymer binder, but too many zeolites in a homogeneous semi-amorphous geopolymer gel structure may contribute to a weakly bonded geopolymer structure, which may lead to a reduction in strength. As crystallisation continues between Day 7 and Day 200, a decrease in strength is obs.

To characterise the structural changes of the raw material during the geopolymerisation process, FTIR spectral curves have been taken for both the metakaolin and the obtained binders (Fig. 4.16 and Table 4.6). The transmittance spectra of metakaolin are characterised by two intense main peaks, at 1087 cm^{-1}, characteristic of asymmetric stretching vibrations of the T-O (where T is Si or Al) bands, and at 456 cm^{-1}, indicative of bending vibrations of the internal T-O bands [79]. After the geopolymerisation process, the peak at 1087 cm^{-1} shifts to 991–1023 cm^{-1} due to the formation of the geopolymer gel [79], [80]. This peak for the samples made with activation solution A4 corresponds to a higher wavenumber after the geopolymerisation process (1020–1023 cm^{-1}) than for the samples made with activation solution A2 (991–1001 cm^{-1}) due to the Si/Al ratio decrease [80], [81]. Peaks at 558–564 cm^{-1} are characteristic of stretching vibrations of tetrahedral aluminium [81], [82]. As shown in Fig. 4.16, for the low-silica activation solution samples (i.e., samples M-R-A2, M-P-A2, M-A-A2), these peaks are more intense than for the high-silica activation solution samples (i.e., samples M-R-A4, M-P-A4, M-A-A4). Considering that M-R-A2, M-P-A2 and M-A-A2 contain a significant amount of zeolite 4A and M-A-A4 contains a small amount of zeolite 4A, no zeolite compounds were found in M-R-A4 and M-A-A4. Therefore it can be argued that the vibrational peaks at 558–564 cm^{-1} of the ligaments in the samples obtained after the geopolymerisation process have become markedly more intense due to the vibration of the double tetrahedral rings in the zeolite grid [73]. All samples demonstrate internal T-O bond bending vibrations at 453–457 cm^{-1} after the geopolymerisation process. An asymmetric stretching vibration of the C-O bonds, characteristic of sodium carbonate in terms of the nature and position of the spectral curve, appears at 1381–1464 cm^{-1} [79], but the bending of the C-O bonds in the plane occurs at 852–877 cm^{-1} [83]. The bands at 1631–1645 cm^{-1} are indicative of O-H band bending vibrations in H_2O molecules [84], [85].

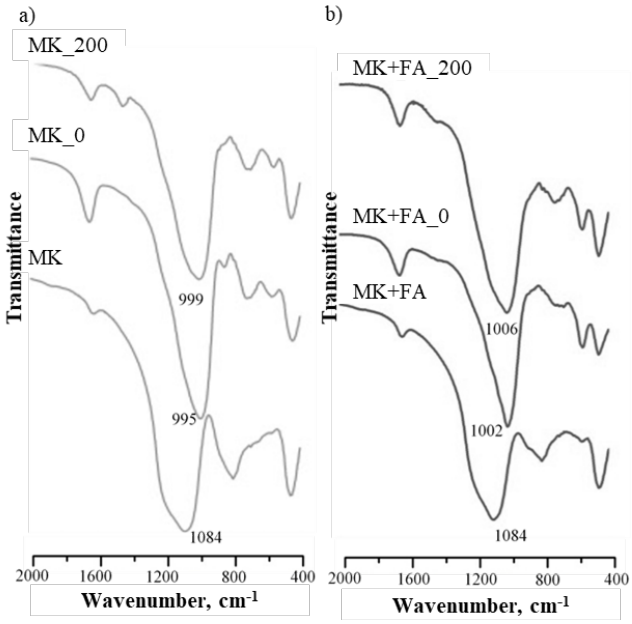

Fig. 4.16. FTIR transmittance spectra of metakaolin and obtained geopolymer binders: a) with low-silica activation solution (activation solution A2); b) with high-silica activation solution (activation solution A4).

Table 4.6

Position and interpretation of peaks in the FTIR transmittance spectra of metakaolin and obtained geopolymer binders

Composition							Interpretation	Ref.
MK	M-R-A2	M-P-A2	M-A-A2	M-R-A4	M-P-A4	M-A-A4		
1631[b]	1643[a]	1639[a]	1639[a]	1642[a]	1645[a]	1637[a]	ν_4 O-H (H_2O)	[84], [85]
-	1403–1459[c]	1381–1464[c]	1395–1459[b]	1382–1455[b]	1393–1455[b]	1387–1457[b]	ν_3 C-O (CO_3^{2-})	[79]
1087[a]	997[a]	991[a]	1001[a]	1022[a]	1020[a]	1023[a]	ν_3 T-O	[80], [81]
-	852[b]	849[b]	857[b]	877[b]	869[b]	874[b]	ν_2 C-O (CO_3^{2-})	[83]
799[a]	799[c]	799[c]	799[c]	799[c]	799[c]	799[c]	ν_1 Si-O	[79]
693[c]	696–720[a]	698–722[a]	699–717[a]	695–713[b]	696–718[b]	696–718[b]	ν_4 Si-O-Si	[79]
566[c]	558[a]	561[a]	559[a]	562[b]	564[b]	562[b]	ν_4 Al-O-Al	[73],[81], [82]
456[a]	457[a]	457[a]	457[a]	453[a]	457[a]	453[a]	ν_4 Si-O	[79], [80]

a – high intensity; b – low intensity; c – very low intensity.

Three compositions (M-A-A2, M-P-A4, and M-A-A4, respectively) were selected from the prepared samples (Table 4.5) to study their micro-structure by scanning electron microscopy (SEM) (Fig. 4.17).

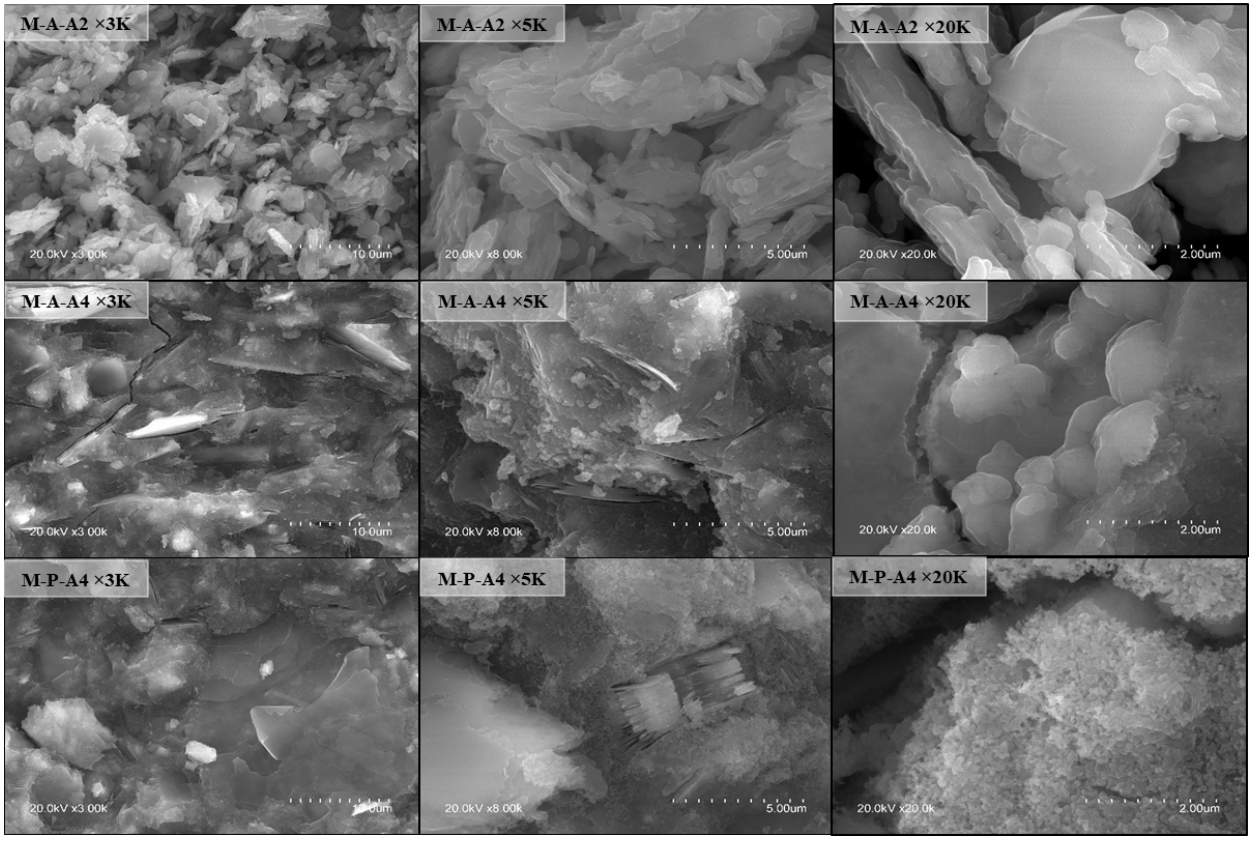

Fig. 4.17. Microphotomicrographs of the structure of the obtained geopolymer binder.

The geopolymer binder M-A-A2 has the lowest material density of the three binders shown in Fig. 4.17. Due to the low silica activation solution (i.e., A2), M-A-A2 does not contain sufficient reactive SiO_2 from the sodium metasilicate containing activation solution to enter the system but uses an increased amount of water to evaporate during the curing process. For this reason, the microstructure of M-A-A2 is not monolithic and there are voids between the particles, resulting in a lower density of the material (Fig. 4.13). The micro-structure of the material at 3000, 5000, and 20000 times magnification is shown in Fig. 4.17. An inhomogeneous structure was observed in M-A-A2 by SEM at 3000 times magnification. The metakaolin platelets have not fully reacted with the activation solution during the geopolymerisation process to form a monolithic geopolymer gel but have reacted to form a gel-like coating and have retained their lamellar morphology. Meanwhile, the structure of M-A-A4 consists essentially of a homogeneous geopolymer gel in which unreacted metakaolin platelets are "incorporated" here and there. In the M-P-A4 structure, clusters of pseudo-hexagonal lamellae are observed, which, according to the literature, correspond to crystals of the kaolin mineral [86].

4.5.Compatibility of geopolymer binders and bio-fillers

To improve the sustainability of geopolymer-based materials, geopolymer binders can be combined with environmentally friendly fillers, i.e., plant-based fillers or bio-fillers obtained as by-products. Bio-based fillers such as hemp shives, flax shive, oat husks and wood chips obtained as by-products of production are considered as sustainable fillers to produce alternative materials. Hemp shive has become a common filler for bio-composites due to its porous structure and suitable thermal properties. This section of the study focuses on the suitability of geopolymer binders for the production of bio-composites.

Sample preparation

A metakaolin-based geopolymer binder has been chosen for the biocomposites, which is made using an 8M NaOH solution (A1). For the bio-composite samples, the geopolymer binder first is mixed and then covered with a polyethylene film and left for 1 h. A specific amount of the geopolymer binder (i.e., 2.0 wt%, 3.0 wt% or 4.0 wt%) is added to the wet hemp shive (1.0 wt% dry hemp sihve mixed with 1.0 wt% water) and mixed manually until a homogeneous structure is obtained (~5 min). The resulting fresh material is filled into moulds and covered with a polyethylene film, after which the sample is compressed to the required height (50 mm) using threaded rods, rod washers and spacers. The material is pressed under pressure for 30 min and then placed in an oven at 85 °C for 24 h.

Results

Figure 4.18 shows the material density and compressive strength results of the obtained geopolymer binder-based bio-composite material. The bio-composite has a material density ranging from 261 kg/m^3 to 403 kg/m^3. As can be seen in Fig. 4.18, the material density depends on the geopolymer binder/hemp shive ratio, while the type of hemp shive has no significant effect on the material density. Increasing the geopolymer binder/hemp shive ratio by a factor

of two (i.e., from 2.0 to 4.0) increases the material density by 54.4 % for BC-A and by 52.3 % for BC-B.

The obtained bio-composites show a compressive strength of up to 0.48 MPa on Day 28. As shown in Fig. 4.18 a), the bio-composites with a geopolymer binder/hemp shive ratio of 2.0 have a compressive strength lower than 0.10 MPa. As expected, increasing the ratio of geopolymer binder to hemp shive increases the compressive strength of the resulting bio-composite. The bio-composites with hemp shive A show slightly higher compressive strength compared to the bio-composites with hemp bundle B.

The thermal conductivity of the obtained bio-composites, depending on the geopolymer binder/hemp shive ratio, is shown in Fig. 4.18 b). Bio-composites with thermal conductivities ranging from 0.061 W/(m·K) to 0.077 W/(m·K) were obtained. Decreasing the geopolymer binder/hemp shive ratio decreases the difference between the bio-composites with different hemp shive (hemp shive A and hemp shive B, respectively). On the other hand, the highest geopolymer binder/hemp shive ratio (4.0) results in a difference of 0.003 (0.074 BC-A-4 and 0.077 BC-B-4), which falls within the measurement error tolerance.

In the case of hemp shive A, when incorporated into geopolymer binder-based bio-composites, the thermal conductivity increases by 42 % at a geopolymer binder/hemp shive ratio of 2.0 and by 72 % at twice the geopolymer binder/hemp shive ratio. Meanwhile, for hemp shive B, the thermal conductivity increases by 36 % to 71 %.

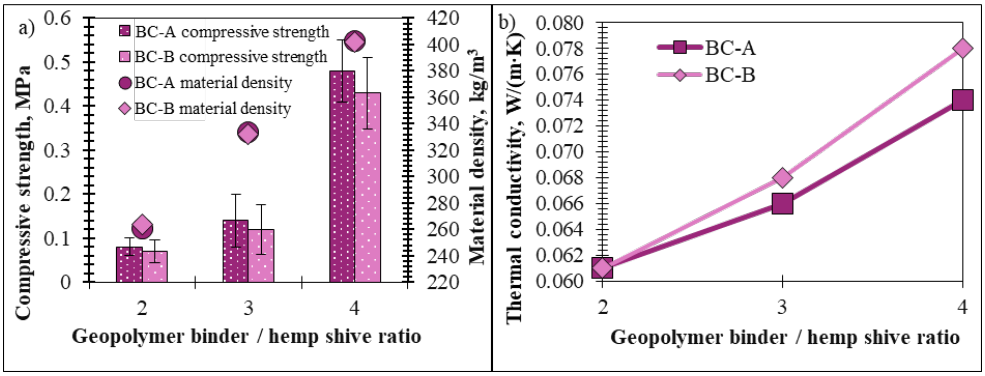

Fig. 4.18. Properties of the obtained bio-composites depending on the geopolymer binder/hemp shive ratio: a) material density and compressive strength; b) thermal conductivity.

L. Liu et. al. have developed geopolymer-based bio-composites with material density ranging from 290 kg/m^3 to 320 kg/m^3, compressive strength of 0.07–1.7 MPa, and thermal conductivity of 0.099–0.120 W/(m·K) [65]. Meanwhile, another alternative bio-composite solution has been proposed by N. Belayachi et al. – gypsum-based bio-composites with material density ranging from 184 kg/m^3 to 456 kg/m^3, compressive strength of 0.004–0.071 MPa and thermal conductivity of 0.058–0.086 W/(m·K) [75]. Comparison of the results obtained in other studies available in the literature shows that the bio-composites produced have an improved thermal conductivity at equivalent material densities.

Figure 4.19 illustrates the macro-structure of the resulting geopolymers. As can be seen from the micro-CT images, the hemp shive in the material is not oriented in the same direction. The hemp particles are uniformly coated with a geopolymer binder, which provides the mechanical strength of the material, and there are voids between them, which, combined with the porous structure of the hemp particles, provide the low thermal conductivity.

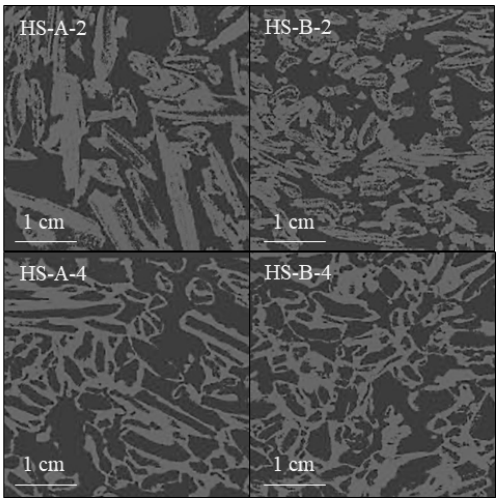

Fig. 4.19. Structure of the obtained bio-composites.

The environmental advantages of natural fillers derived from agricultural waste by-products include biodegradability, renewability, recyclability, composability, and the potential to reduce greenhouse gas emissions. The use of these fillers has the potential to reduce the emissions produced by insulation materials currently on the market, as well as to reduce agricultural waste and make it part of the circular economy [87].

4.6. Sustainability assessment of the developed building materials

The GHG emissions of Portland cement, the most commonly used binder in construction, are 0.866 kg CO_2 eq per kg, while the GHG emissions of the geopolymer binders developed in the study range from 0.458 kg to 0.759 kg CO_2 eq. According to the data, the type of activation solution has a significant effect on the GHG emissions of the geopolymer binders. The choice of 8 M NaOH as the activation solution results in geopolymer binders with GHG emission reductions ranging from 37 % to 43 %. However, replacing the 10 % 8 M NaOH with a sodium metasilicate solution results in a 2 % reduction in GHG emissions, i.e., between 35 % and 41 %.

The choice of alternative binders can reduce the consumption of non-renewable resources by 64–86 %, depending on the composition of the geopolymer binder chosen. The non-renewable resource consumption in the production of geopolymer binders is primarily determined by the aluminium silicate sources used. The choice of a metakolin-based geopolymer binder with an activation solution/dry raw material ratio of 0.92 as an alternative to Portland cement can reduce the non-renewable resource consumption by 81–82 %.

The developed and investigated bio-composites with a material density of 260 kg/m^3 were compared with commercially available building materials such as hard rock wool and foamed glass. In order to make the comparison as objective as possible, the materials are compared with the same U-value of 0.105 W/(m^2·K). According to the results, the production of bio-composites developed in the study use 4.6 times more fossil resources than the production of the rock wool, while 1.5 times less than the production of the foamed glass. Also in terms of GHG emissions, rock wool is a more environmentally friendly option (i.e., 2.4 times lower GHG emissions), while the production of foamed glass has 2.4 times higher GHG emissions compared to the developed bio-composites.

CONCLUSIONS

By varying the initial temperature of the geopolymer binder, the Na/Si ratio, the water/alkali ratio and the mixing time, the workability, physical and mechanical properties of the geopolymer binder can be controlled. By varying one or more of these factors, significant improvements in the properties of the geopolymer binders can be achieved.

Increasing the initial temperature of the raw materials from 5 °C to 35 °C causes changes in the workability of the binder and the curing process. The flowability of the fresh geopolymer binder increases by 14.3 % for the binders with a water/10 M NaOH ratio of 0.6 and by 28.2 % for the binders with a water/10 M NaOH ratio of 1.4. The compressive strength of geopolymer binders made from raw materials with an initial temperature of 5 °C and an activation solution with a water/10 M NaOH ratio of 1.4 increases by a factor of 1.7, and with 0.6 by a factor of 2.0 (after 56 days). Increasing the initial temperature of the raw materials to 15 °C and 35 °C has less effect on the strength after 56 days, i.e., 1.3 times for geopolymer binders with an activation solution of water/10 M NaOH of 1.4 and 1.7 times with 0.6.

By modifying the mixing time of the binder and the optimum SiO_2/Al_2O_3 ratio, activation solution to metakaolin ratio (AS/MK), the spread diameter and mechanical strength of the geopolymer binder can be controlled. The optimum SiO_2/Al_2O_3 ratio of 1.6 and activation solution to metakaolin ratio (AS/MK) of 0.7 can provide a fresh geopolymer binder with a flowability (spread diameter >180 mm) and compressive strength at Day 3 >7 MPa. 3 min of mixing of the metackolin-based geopolymer binder is the optimum mixing time in terms of flowability and compressive strength of the cured geopolymer binder.

The activation solution has a significant effect on the compressive strength of the geopolymer binder. By reducing the amount of water in the activation solution, the density of the metakaolin-based geopolymer binder material increases relatively slightly (i.e., from 1510 kg/m^3 to 1530 kg/m^3), but the compressive strength increases threefold (i.e., from 5.1–6.7 MPa to 16.3–20 MPa). The initial raw material temperature affects the early bond strength and the rate of strength increase at constant geopolymer binder composition but does not affect the final strength.

In order to ensure a stable structure of the geopolymer binder and to minimise leaching of salts when the material comes into contact with water, it is recommended to use metakaolin-based raw materials for the geopolymer binder. Heat post-treatment at 200 °C significantly reduces the risk of salinisation.

The density, mechanical strength, mineralogical and structural properties of the resulting geopolymer binder material depend on the type of activation solution used (low or high silica content) and the likelihood of the formation of zeolite crystals in the geopolymer structure. The chemical composition of the raw materials (aluminium silicate sources) as well as the SiO_2/Na_2O and Al_2O_3/Na_2O ratios in the raw materials determine the rate of formation, type, size and amount of zeolites in the geopolymer structure.

To limit the formation of zeolite crystals in the geopolymer structure, it is recommended to use an activation solution with a high silicon content, so that crystalline compounds do not form in the geopolymer binder structure during curing but the geopolymer gel continues to develop.

Replacing Portland cement, which is widely used in construction, with alternative geopolymer binders can reduce GHG emissions by 12–47 % and non-renewable resource consumption by 64–86 %.

For geopolymer binder-based bio-composites, the ratio of geopolymer binder to hemp shive shall be at least 3.0 for a compressive strength >0.05 MPa and at least 4.0 for >0.25 MPa. The type of hemp shive used shall not significantly affect the properties of the geopolymer binder-based bio-composites produced. The geopolymer binder can be used in combination with hemp shive to produce bio-composites, resulting in a self-supporting building material with a material density of 260–400 kg/m^3, compressive strength up to 0.26 MPa, and a thermal conductivity of 0.061–0.077 W/(m·K).

REFERENCES

[1] Communication from the Commission to the European Parliament, the European Council, the Council, the European Economic and Social Committee and the Committee of the Regions - A European Green Deal- Publications Office of the EU." Available: https://op.europa.eu/publication-detail/-/publication/b828d165-1c22-11ea-8c1f-01aa75ed71a1/language-lv [accessed 24.03.2022.].

[2] P. Koltun, Materials and sustainable development, Progress in Natural Science: Materials International, vol. 20, no. 1, pp. 16–29, Nov. 2010, doi: 10.1016/S1002-0071(12)60002-1.

[3] P. A. Owusu, S. Asumadu-Sarkodie, A review of renewable energy sources, sustainability issues and climate changemitigation, Cogent Engineering, vol. 3, no. 1, 2016, doi: 10.1080/23311916.2016.1167990.

[4] S. Usha, N, G., Deepa, S. Vishnudas, Geopolymer binder from industrial wastes: a review, IJCIET. 5. 219-225, 2014.

[5] M. Qu, S. Hamdani, J. A. Bunce, The physiology and genetics of stomatal adjustment under fluctuating and stressed environments, Applied Photosynthesis - New Progress, 2016, doi: 10.5772/62223.

[6] M. V. Madurwar, R. V. Ralegaonkar, S. A. Mandavgane, Application of agro-waste for sustainable construction materials: A review, Constr Build Mater, vol. 38, pp. 872–878, 2013, doi: 10.1016/J.CONBUILDMAT.2012.09.011.

[7] A. Mohajerani, D. Suter, T. Jeffrey-Bailey, T. Song, A. Arulrajah, S. Horpibulsuk, D. Law, Recycling waste materials in geopolymer concrete, Clean Technologies and Environmental Policy 2019 21:3, vol. 21, no. 3, pp. 493–515, 2019, doi: 10.1007/S10098-018-01660-2.

[8] Utsläpp av växthusgaser från bygg- och fastighetssektorn - Boverket. Available: https://www.boverket.se/sv/byggande/hallbart-byggande-och-forvaltning/miljoindikatorer---aktuell-status/vaxthusgaser/ [accessed 30.03.2022.].

[9] E. Hertwich., R. Lifset, S. Pauliuk, N. Heeren, S. Ali, Q. Tu, F. Ardente, P. Berrill, T. Fishman, K. Kanaoka, J. Kulczycka, T. Makov, E. Masanet, P. Wolfram, Resource Efficiency and Climate Change: Material Efficiency Strategies for a Low-Carbon Future. Zenodo, 2019, https://doi.org/10.5281/zenodo.5245528

[10] M. Norouzi, M. Chafer, L. F. Cabeza, L. Jimenez, and D. Boer, Circular economy in the building and construction sector: A scientific evolution analysis, Journal of Building Engineering, vol. 44, p. 102704, 2021, doi: 10.1016/J.JOBE.2021.102704.

[11] S. Geng, Y. Wang, J. Zuo, Z. Zhou, H. Du, and G. Mao, Building life cycle assessment research: A review by bibliometric analysis, Renewable and Sustainable Energy Reviews, vol. 76, pp. 176–184, 2017, doi: 10.1016/J.RSER.2017.03.068.

[12] N. Mohamad, K. Muthusamy, R. Embong, A. Kusbiantoro, and M. H. Hashim, Environmental impact of cement production and Solutions: A review, Mater Today Proc, vol. 48, pp. 741–746, 2022, doi: 10.1016/J.MATPR.2021.02.212.

[13] H. Ulusu, H. Y. Aruntas, and O. Gencel, Investigation on characteristics of blended cements containing pumice, Constr Build Mater, vol. 118, pp. 11–19, 2016, doi: 10.1016/J.CONBUILDMAT.2016.05.030.

[14] M. H. Raza and R. Y. Zhong, A sustainable roadmap for additive manufacturing using geopolymers in construction industry, Resour Conserv Recycl, vol. 186, p. 106592, 2022, doi: 10.1016/J.RESCONREC.2022.106592.

[15] V. Shobeiri, B. Bennett, T. Xie, and P. Visintin, A comprehensive assessment of the global warming potential of geopolymer concrete, J Clean Prod, vol. 297, p. 126669, 2021, doi: 10.1016/J.JCLEPRO.2021.126669.

[16] N. Shehata, O. A. Mohamed, E. T. Sayed, M. A. Abdelkareem, and A. G. Olabi, Geopolymer concrete as green building materials: Recent applications, sustainable development and circular economy potentials, Science of The Total Environment, vol. 836, p. 155577, 2022, doi: 10.1016/J.SCITOTENV.2022.155577.

[17] Z. Emdadi, N. Asim, M. H. Amin, M. A. Yarmo, A. Maleki, M. Azizi, K.Sopian, Development of Green Geopolymer Using Agricultural and Industrial Waste Materials with High Water Absorbency, Applied Sciences 2017, Vol. 7, Page 514, vol. 7, no. 5, p. 514, 2017, doi: 10.3390/APP7050514.

[18] M. Sumesh, U. J. Alengaram, M. Z. Jumaat, K. H. Mo, M. F. Alnahhal, Incorporation of nano-materials in cement composite and geopolymer based paste and mortar – A review, Constr Build Mater, vol. 148, pp. 62–84, 2017, doi: 10.1016/J.CONBUILDMAT.2017.04.206.

[19] J. Davidovits, Geopolymer Cement a review, Geopolymer Science and Technics, no. 0, pp. 1–11, 2013.

[20] J. L. Provis, Geopolymers and other alkali activated materials: why, how, and what?, Mater Struct, vol. 47, pp. 11–25, 2014, doi: 10.1617/s11527-013-0211-5.

[21] A. Passuello, Evaluation of the potential improvement in the environmental footprint of geopolymers using waste-derived activators, J Clean Prod, 2017, doi: 10.1016/j.jclepro.2017.08.007.

[22] UNI1987: Brundtland Report. Available: https://www.are.admin.ch/are/en/home/media/publications

/sustainable-development/brundtland-report.html [accessed 3.04.2023.].

[23] UNEP 2009 annual report. UNEP - UN Environment Programme. Available: https://www.unep.org/resources/annual-report/unep-2009-annual-report [skatīts 3.04.2023.]

[24] S. Amziane, L. Arnaud, Bio-aggregate-based Building Materials, 2017, doi: 10.1007/978-94-024-1031-0

[25] M. Asif, T. Muneer, R. Kelley, Life cycle assessment: A case study of a dwelling home in Scotland, Build Environ, vol. 42, no. 3, pp. 1391–1394, 2007, doi: 10.1016/J.BUILDENV.2005.11.023.

[26] The European Green Deal must be at the heart of the COVID-19 recovery. World Economic Forum. Available: https://www.weforum.org/agenda/2020/05/the-european-green-deal-must-be-at-the-heart-of-the-covid-19-recovery/ [accessed 16.03.2023].

[27] Impacts of circular economy policies on the labour market - Publications Office of the EU. Available: https://op.europa.eu/en/publication-detail/-/publication/fc373862-704d-11e8-9483-01aa75ed71a1/language-en [accessed 30.03.2022].

[28] X. Zhao, J. Zuo, G. Wu, C. Huang, A bibliometric review of green building research 2000–2016, https://doi.org/10.1080/00038628.2018.1485548, vol. 62, no. 1, pp. 74–88, 2018, doi: 10.1080/00038628.2018.1485548.

[29] L. Perez-Lombard, J. Ortiz, C. Pout, A review on buildings energy consumption information, Energy Build, vol. 40, no. 3, pp. 394–398, 2008, doi: 10.1016/J.ENBUILD.2007.03.007.

[30] J. Zuo, Z. Y. Zhao, "Green building research–current status and future agenda: A review, Renewable and Sustainable Energy Reviews, vol. 30, pp. 271–281, 2014, doi: 10.1016/J.RSER.2013.10.021.

[31] Why The Building Sector? – Architecture 2030. Available: https://architecture2030.org/why-the-building-sector/ [accessed 16.03.2022.].

[32] L. Verdolotti, S. Colini, G. Porta, S. Iannace, Effects of the addition of LiCl, LiClO4, and LiCF3SO3 salts on the chemical structure, density, electrical, and mechanical properties of rigid polyurethane foam composite, Polym Eng Sci, vol. 51, no. 6, pp. 1137–1144, 2011, doi: 10.1002/PEN.21846.

[33] L. K. Turner, F. G. Collins, Carbon dioxide equivalent (CO2-e) emissions: A comparison between geopolymer and OPC cement concrete," Constr Build Mater, vol. 43, pp. 125–130, 2013, doi: 10.1016/J.CONBUILDMAT.2013.01.023.

[34] B. Panda, S. C. Paul, L. J. Hui, Y. W. D. Tay, M. J. Tan, "Additive manufacturing of geopolymer for sustainable built environment," J Clean Prod, vol. 167, pp. 281–288, 2017, doi: 10.1016/J.JCLEPRO.2017.08.165.

[35] A. Hassan, M. Arif, M. Shariq, "Use of geopolymer concrete for a cleaner and sustainable environment – A review of mechanical properties and microstructure," J Clean Prod, vol. 223, pp. 704–728, 2019, doi: 10.1016/J.JCLEPRO.2019.03.051.

[36] L. N. Assi, K. Carter, E. Deaver, P. Ziehl, "Review of availability of source materials for geopolymer/sustainable concrete," J Clean Prod, vol. 263, p. 121477, 2020, doi: 10.1016/J.JCLEPRO.2020.121477.

[37] F. Pacheco-Torgal, J. Castro-Gomes, S. Jalali, Alkali-activated binders : A review Part 1 . Historical background , terminology , reaction mechanisms and hydration products, Constr Build Mater, vol. 22, pp. 1305–1314, 2008, doi: 10.1016/j.conbuildmat.2007.10.015.

[38] N. N. Shalobyta, V. V. Tur, T. P. Shalobyta, V. I. Rakhuba, ENERGY EFFICIENT COMPOSITES USING NATURAL ORGANIC MATERIALS, in E3S Web of Conferences, 2019, doi: 10.1051/e3sconf/201913602027.

[39] A. Arrigoni, R. Pelosato, P. Meli, G. Ruggieri, S. Sabbadini, G. Dotelli, Life cycle assessment of natural building materials: the role of carbonation, mixture components and transport in the environmental impacts of hempcrete blocks, J Clean Prod, vol. 149, pp. 1051–1061, 2017, doi: 10.1016/j.jclepro.2017.02.161.

[40] G. Bumanis, L. Vitola, I. Pundiene, M. Sinka, and D. Bajare, Gypsum, geopolymers, and starch-alternative binders for bio-based building materials: A review and life-cycle assessment, Sustainability, vol. 12, no. 14, 2020, doi: 10.3390/SU12145666.

[41] G. Furtos, L. Silaghi-Dumitrescu, P. Pascuta, C. Sarosi, K. Korniejenko, Mechanical Properties of Wood Fiber Reinforced Geopolymer Composites with Sand Addition, Journal of Natural Fibers, vol. 0, no. 0, pp. 1–12, 2019, doi: 10.1080/15440478.2019.1621792.

[42] Z. Li, S. Li, Effects of wetting and drying on alkalinity and strength of fly ash/slag-activated materials, Constr Build Mater, vol. 254, p. 119069, 2020, doi: 10.1016/j.conbuildmat.2020.119069.

[43] C. Leiggener, A. Currao, G. Calzaferri, Zeolite A and ZK-4, in Materials Syntheses: A Practical Guide, 2008, pp. 21–28. doi: 10.1007/978-3-211-75125-1_2.

[44] Y.-S. Yoo, K.-H. Cheon, J.-I. Lee, B.-S. Kim, W.-S. Shin, G.-T. Seo, Zeolite synthesis using sewage sludge by molten-salt method, vol. 569. 2008. doi: 10.4028/0-87849-472-3.329.

[45] R. Wang, J. Wang, T. Dong, G. Ouyang, Structural and mechanical properties of geopolymers made of aluminosilicate powder with different SiO2/Al2O3 ratio: Molecular dynamics simulation and microstructural experimental study, Constr Build Mater, 2020, doi: 10.1016/j.conbuildmat.2019.117935.

[46] S. K. Pitcher, R. C. T. Slade, N. I. Ward, Heavy metal removal from motorway stormwater using zeolites, Science of the Total Environment, vol. 334–335, pp. 161–166, 2004, doi: 10.1016/j.scitotenv.2004.04.035.

[47] F. Plana, Synthesis of zeolites from ash at pilot plant scale . Examples of potential applications, vol. 80, 2001.

[48] I. Garcia-Lodeiro, A. Palomo, A. Fernández-Jiménez, D. E. Macphee, Compatibility studies between N-A-S-H and C-A-S-H gels. Study in the ternary diagram Na2O–CaO–Al2O3–SiO2–H2O, Cem Concr Res, vol. 41, no. 9, pp. 923–931, 2011, doi: 10.1016/j.cemconres.2011.05.006.

[49] A. Palomo, I. Sobrados, J. Sanz, M. Criado, A. Ferna, Effect of the SiO2/Na2O ratio on the alkali activation of fly ash . Part II : Si MAS-NMR Survey, vol. 109, pp. 525–534, 2008, doi: 10.1016/j.micromeso.2007.05.062.

[50] A. Fernandez-Jimenez, A. G. de la Torre, A. Palomo, G. Lopez-Olmo, M. M. Alonso, M. A. G. Aranda, Quantitative determination of phases in the alkaline activation of fly ash. Part II: Degree of reaction, Fuel, vol. 85, no. 14–15, pp. 1960–1969, 2006, doi: 10.1016/j.fuel.2006.04.006.

[51] A. Macias, S. Goni, J. Madrid, Limitations of Koch-Steinegger test to evaluate the durability of cement pastes in acid medium, Cem Concr Res, vol. 29, no. 12, pp. 2009.

[52] G. Bumanis, L. Vitola, D. Bajare, L. Dembovska, I. Pundiene, Impact of reactive SiO2/Al2O3 ratio in precursor on durability of porous alkali activated materials, Ceram Int, vol. 43, no. 7, pp. 5471–5477, 2017, doi: 10.1016/j.ceramint.2017.01.060.

[53] R. Wachter, J. Barthel, Untersuchungen zur Temperaturabhängigkeit der Eigenschaften von Elektrolytlösungen II. Bestimmung der Leitfähigkeit über einen großen Temperaturbereich, Berichte der Bunsengesellschaft für physikalische Chemie, 1979, doi: 10.1002/bbpc.19790830618.

[54] A. Usobiaga, A. De Diego, J. M. Madariaga, Electrical conductivity of concentrated aqueous mixtures of HCl and KCl in a wide range of compositions and temperatures, J Chem Eng Data, 2000, doi: 10.1021/je990160u.

[55] D. W. Zhang, D. Min Wang, Z. Liu, F. Zhu Xie, Rheology, agglomerate structure, and particle shape of fresh geopolymer pastes with different NaOH activators content, Constr Build Mater, 2018, doi: 10.1016/j.conbuildmat.2018.07.205.

[56] G. Ishwarya, B. Singh, S. Deshwal, S. K. Bhattacharyya, Effect of sodium carbonate/sodium silicate activator on the rheology, geopolymerization and strength of fly ash/slag geopolymer pastes, Cem Concr Compos, vol. 97, pp. 226–238, 2019, doi: 10.1016/j.cemconcomp.2018.12.007.

[57] C. Ruiz-Santaquiteria, A. Fernandez-Jimenez, J. Skibsted, A. Palomo, Clay reactivity: Production of alkali activated cements, Appl Clay Sci, vol. 73, no. 1, pp. 11–16, 2013, doi: 10.1016/j.clay.2012.10.012.

[58] F. Pacheco-Torgal, J. A. Labrincha, C. Leonelli, A. Palomo, P. Chindaprasirt, Handbook of Alkali-Activated Cements, Mortars and Concretes. 2014. doi: 10.1016/C2013-0-16511-7.

[59] A. Fernandez-Jimenez, I. García-Lodeiro, A. Palomo, Durability of alkali-activated fly ash cementitious materials, J Mater Sci, vol. 42, no. 9, pp. 3055–3065, 2007, doi: 10.1007/s10853-006-0584-8.

[60] G. Bumanis, L. Vitola, A. Fernandez-Jimenez, A. Palomo, D. Bajare, The Effect of Heat Treatment on Alkali Activated Materials, Materials Science (Medžiagotyra), vol. 23, no. 3, pp. 266–272, 2017.

[61] X. Querol, Synthesis of zeolites from coal fly ash: an overview, Int J Coal Geol, vol. 50, no. 1–4, pp. 413–423, 2002, doi: 10.1016/S0166-5162(02)00124-6.

[62] Z. Zhang, H. Wang, J. L. Provis, F. Bullen, A. Reid, Y. Zhu, Quantitative kinetic and structural analysis of geopolymers. Part 1. the activation of metakaolin with sodium hydroxide, Thermochim Acta, vol. 539, pp. 23–33, 2012, doi: 10.1016/j.tca.2012.03.021.

[63] A. Ferna, Composition and microstructure of alkali activated fly ash binder : Effect of the activator, vol. 35, pp. 1984–1992, 2005, doi: 10.1016/j.cemconres.2005.03.003.

[64] I. Garcia-Lodeiro, A. Fernandez-Jimenez, M. T. Blanco, A. Palomo, FTIR study of the sol-gel synthesis of cementitious gels: C-S-H and N-A-S-H," J Solgel Sci Technol, vol. 45, no. 1, pp. 63–72, 2008, doi: 10.1007/s10971-007-1643-6.

[65] A. Criado, M. Palomo, A. Fernandez-Jimenez, Alkali activation of fly ashes. Part 1: Effect of curing conditions on the carbonation of the reaction products, Fuel, vol. 84, no. 16, pp. 2048–2054, 2005, doi: 10.1016/j.fuel.2005.03.030.

[66] W. K. W. Lee, J. S. J. Van Deventer, Use of Infrared Spectroscopy to Study Geopolymerization of Heterogeneous Amorphous Aluminosilicates, Langmuir, vol. 19, no. 21, pp. 8726–8734, 2003, doi: 10.1021/la026127e.

[67] A. Fernandez-Jimenez, A. Palomo, Mid-infrared spectroscopic studies of alkali-activated fly ash structure, Microporous and Mesoporous Materials, vol. 86, no. 1–3, pp. 207–214, 2005, doi: 10.1016/j.micromeso.2005.05.057.

[68] J. Minkiewicz, W. Mozgawa, M. Kr, IR spectroscopy studies of zeolites in geopolymeric materials derived from kaolinite, vol. 1126, pp. 200–206, 2016, doi: 10.1016/j.molstruc.2016.02.027.

[69] M. J. Genge, A. P. Jones, and G. D. Price, An infrared and Raman study of carbonate glasses: implications for the structure of carbonatite magmas, Geochim Cosmochim Acta, vol. 59, no. 5, pp. 927–937, 1995, doi: 10.1016/0016-7037(95)00010-0.

[70] J. Minkiewicz, W. Mozgawa, M. Kr, IR spectroscopy studies of zeolites in geopolymeric materials derived from kaolinite, vol. 1126, pp. 200–206, 2016, doi: 10.1016/j.molstruc.2016.02.027.

[71] W. Rondon, Application of 3A Zeolite Prepared from Venezuelan Kaolin for Removal of Pb (II) from Wastewater and Its Determination by Flame Atomic Absorption Spectrometry, Am J Analyt Chem, vol. 04, no. 10, pp. 584–593, 2013, doi: 10.4236/ajac.2013.410069.

[72] H. Mahmood, M. Moniruzzaman, S. Yusup, N. Muhammad, T. Iqbal, H. M. Akil, Ionic liquids pretreatment for fabrication of agro-residue/thermoplastic starch based composites: A comparative study with other pretreatment technologies, J Clean Prod, vol. 161, pp. 257–266, 2017, doi: 10.1016/J.JCLEPRO.2017.05.110.

Laura Vītola was born in 1993 in Priekule. She received a Professional Bachelor's degree and an engineering qualification in Civil Engineering in 2017 and a Professional Master's degree in Civil Engineering in 2018 from Riga Technical University. From 2014–2019, she was a research assistant and, since 2019, a researcher at the Institute of Materials and Structures of RTU Faculty of Civil Engineering.
Laura has been on internships at foreign research institutions, including the Concrete Technology Laboratory of Vilnius Gediminas Technical University (Vilnius, Lithuania), Faculty of Civil Engineering and Architecture of Kaunas University of Technology (Kaunas, Lithuania), Eduardo Torroja Institute of Construction Sciences (Madrid, Spain), and the Department of Civil and Environmental Engineering of Brunel University (London, UK). In 2022, Laura was awarded the L`ORÉAL-UNESCO Women in Science Award.